EPJ Web of Conferences **30**, 05002 (2012)
DOI: 10.1051/epjconf/20123005002

energie atomique • energies alternatives

UNIVERSITÉ DE VERSAILLES ST-QUENTIN-EN-YVELINES

UNIVERSITÉ PARIS SUD
Comprendre le monde, construire l'avenir®

Experiment and Modelling in Structural NMR

November 28th – December 2nd 2011
INSTN – CEA Saclay, France

Nicolas Giraud
Université Paris-sud, France

Fast NMR

[05002]

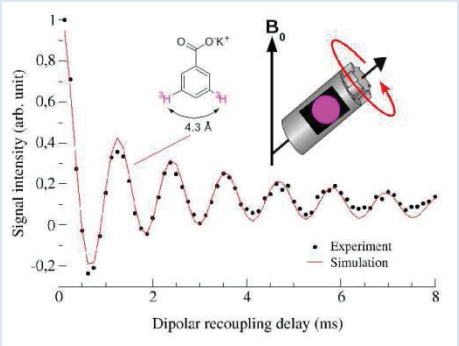

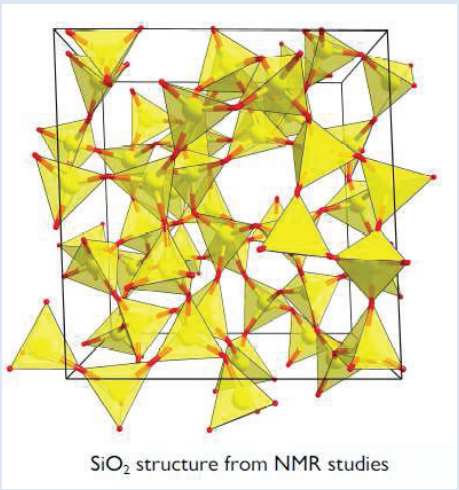
SiO_2 structure from NMR studies

Organized by

Thibault Charpentier thibault.chapentier@cea.fr
Patrick Berthault patrick.berthault@cea.fr
Constantin Meis constantin.meis@cea.fr

Article available at http://www.epj-conferences.org or http://dx.doi.org/10.1051/epjconf/20123005002

Fast NMR

N. Giraud[1]

[1] Equipe de RMN en milieu orienté, ICMMO, UMR 8182 CNRS, Université Paris-Sud, bât 410, 91405 Orsay cedex, France.

Abstract. Three major contributions to the field of Fast NMR techniques are presented. They aim at allowing chemists or biologists to probe structural changes occurring in their sample, on a time scale that is adapted to the observation, the description and the understanding of the (bio)chemical processes under study: (i) the SOFAST approach has been developed to acquire experiments on macromolecules with a high acquisition rate, when band-selective excitation schemes are used; (ii) ultrafast NMR allows to record multi-dimensional spectra within a single scan; and (iii) in gradient frequency encoded NMR, the higher resolution of the correlation spectra makes a straightforward assignment and measurement of spin interactions possible, which leads to an acceleration of the whole analytical process.

1 Introduction

Nuclear Magnetic Resonance has become a particularly well-suited spectroscopy for observing, describing and understanding structure, dynamics and ever more complex reactivity of the molecules that are of the greatest interest nowadays. Most of the methodological developments that have been accomplished over the last 50 years have aimed at pushing the limits of NMR sequences in terms of resolution and acquisition rate.

In this context, multidimensional experiments have proved to be essential to high-resolution studies of large or complex molecular assemblies, in which the observation of resolved correlations provides a detailed insight into their structure, at an atomic level. Unfortunately, the time needed to acquire these multidimensional datasets is a major limitation that prevents scientists from using the NMR spectrum as snapshot of the molecule when it is involved in a dynamic process. Indeed, even in the case of slow processes (protein folding, exchange reaction …), the time scale of these chemical events is not suitable for monitoring structural changes through the variations of correlations on a 2D spectrum.

Along the last decades, several groups have taken up the challenge for shortening the experimental time required to record 2D (3D, 4D …) spectra. Different approaches have been successfully introduced since then, ranging from a shortening of the duration of each scan (SOFAST …) to a reduction of the number of scans needed to sample time domain (non-linear data sampling, Hadamard NMR spectroscopy, parallel acquisition …).

This lecture will focus on three contributions made in the field of Fast NMR: (i) SOFAST spectroscopy, (ii) ultrafast (or single scan) NMR, and (iii) gradient encoded spectroscopy (gNMR).

2 SOFAST NMR

One major limitation on the overall time required to record a multidimensional experiment is the duration of the recycling time that is needed to acquire the NMR signal, and then let the magnetization return to equilibrium before the next scan. For a given experiment, the sensitivity is limited by the fraction of the initial longitudinal magnetization that is converted into transverse coherences that will evolve during the pulse sequence, and the ability of the observed nucleus to relax in a time that is short enough, regarding the desired acquisition rate.[1]

In 2005, Brutscher et al. have made an ingenious use of the relaxation properties of macromolecules, in the frame of correlation experiments based on the use of selective irradiations schemes.[2] In large molecular assemblies such as proteins, the dense proton network offers particularly efficient magnetization transfer pathways (spin diffusion, exchange with water, cross relaxation …) that add to the classical nuclear relaxation mechanisms (spin-lattice relaxation which is basically sensitive to the stochastic fluctuations of spin interactions induced by molecular dynamics). For macromolecules in solution, they have shown that a longitudinal relaxation enhancement is observed, that leads to shorter apparent T_1's for amide protons when these nuclei are selectively excited.

They have thus proposed to implement sequences in which the initial polarization step is built with selective pulses, in order to acquire correlation spectra involving amide protons from proteins on the time scale of few seconds.[3] The resulting SOFAST-HMQC experiment (SOFAST : band-Selective Optimized Flip-Angle Short-Transient) allowed for instance a real-time investigation of a proton/deuterium exchange process in small proteins dissolved in deuterated water.[3, 4]

It has to be noted that in this approach, the flip angle of the initial selective excitation pulse can be optimized so that either a higher sensitivity (BEST sequences), or a shorter recycling delay (SOFAST sequences) is achieved.

This fast-pulsing approach has also been implemented in 3D correlation experiments designed for the measurement of residual dipolar couplings, that allow the rapid measurement of RDC's within a few hours, opening the way to an incorporation of these precious structural probes into computational protocols, and thus a more efficient determination of protein folding within a reduced computation time. [5]

3 Ultrafast NMR

Ultrafast NMR[6] (also known as single-scan NMR) has revolutionized the way of acquiring multidimensional experiments. Indeed, the observation of correlations on a spectrum requires that the evolution of nuclear magnetization be recorded during (at least) two independent evolution delays in the pulse sequence. In a conventional 2D NMR experiment for instance, the indirect domain is sampled over the acquisition of the same 1D experiment repeated N times, each time varying an indirect evolution time (t_1).[7] In this classical approach, the overall acquisition time is proportional to the number N of t_1 increments needed to sample evolution frequencies with a satisfying resolution. This acquisition scheme can result in very long experimental times (up to a few days).

Ultrafast NMR consists in acquiring simultaneously these N experiments (*i.e.* corresponding to each t_1 increment) in different "slices" of the NMR sample.[8] In a way that is similar to Magnetic Resonance Imaging (MRI) techniques, the sample is spatially encoded by a pulsed field gradient. The evolutions of spin nuclei that are located in different cross sections are then triggered one after the other by an adequate frequency swept irradiation scheme, leading to a spatial encoding of the corresponding (indirect) evolution time. This protocol allows a single receiver coil to perform a parallel acquisition of all the signals that were generated with different t_1 increments. After these initial excitation and evolution steps, single-scan 2D pulse sequences are followed by the appropriate mixing block, and finally by a detection of the NMR signal (similarly to classical multi-dimensional sequences). The resulting NMR signal has a double (t_1, t_2) dependency, and needs thus to be decoded. During detection, decoding gradients are then applied, that induce a position dependent phase for nuclear spins along the sample. Over the acquisition time, this generates a refocusing of parts of the magnetization that have been evolving at a given resonance frequency Ω during t_1, at times that are proportional to Ω. The spectrum along the indirect domain is thus directly reconstructed in the final signal, and takes the form of a series of echoes that still contain a time dependence (according to spin evolutions during the acquisition delay t_2). A single Fourier transform along t_2 is then required to obtain the desired 2D spectrum. [8]

Over the recent years, different methodological developments have been devoted to the enhancement of this technique. The excitation scheme, which was originally composed of a train of bipolar gradients and frequency selective pulses to create a *discrete* series of "slices" with different evolution times t_1, has been completed with an alternative scheme employing adiabatic pulses to generate a *continuous* spatial encoding of t_1.[9, 10] Novel acquisition strategies, consisting for instance in interleaving scans, have also been proposed to enhance both resolution and sensitivity. More recently, several approaches have been proposed, that range from excitation schemes allowing to encode a continuous phase modulation of the signal along the sample[11], J-resolved detection schemes[12], to the combination of the ultrafast approach with *ex situ* dynamic nuclear polarization (DNP) techniques.[13] These developments have allowed to implement most of the classical homonuclear correlation spectra (COSY, TOCSY, J-resolved …), as well as heteronuclear experiments (HMQC, HSQC …) that have become essential to any NMR study, in particular in the field of biological macromolecules.[13]

The substantial gain in acquisition rate promised by this methodology has encouraged several groups to write single-scan versions of their pulse programs in order to observe, sometimes at Hertz rate, dynamic events involved in their chemical or biological systems. New applications have been successfully developed, that range from the study of the fast hydrogen-deuterium exchange characterizing amide sites in small model proteins[14], real-time monitoring of organic reactions[15], or the accurate quantification of isotopic enrichments in mixtures of metabolites.[16, 17] Finally, ultrafast NMR could in the future be the key to noticeable evolutions in the field of magnetic resonance imaging itself. Frydman and his co-workers have shown that this approach allows potentially extracting from each voxel sampled during an MRI experiment the spectroscopic information (i.e. the *chemical shift*) that is associated to molecules that are present in the analysed tissues.[18]

4 Gradient frequency-encoded (gNMR) spectroscopy

If ultrafast NMR can be defined as corresponding to a spatial *time* encoding of the sample, another approach relying on a spatial *frequency* encoding has paved the way to a novel generation of experiments with high analytical potential.

Since the advent of Fourier transform NMR, and the development of multidimensional experiments, a vast number of pulse sequences have been specifically

designed, that allow gathering all the interactions between active nuclei together on the same correlation spectrum. However, even for rather small compounds, the overlap of signals, as well as the complexity of their multiplet structure, can overwhelm the resolution of the correlation spectra.

The resolution of any NMR spectrum relies heavily on the action of the pulse sequence on spin dynamics. Remarkably, this property depends above all on the kind of radiofrequency fields that are applied to handle nuclear magnetization, whatever the detail of the pulse sequence is.[19, 20]

On the one hand, sequences which employ hard pulses (short, high power radiofrequency fields) can be designed so that they give rise to different evolutions for different kinds of interactions in the spin network (chemical shift, dipolar or scalar coupling …).[21-24] Unfortunately, the use of hard pulses creates as many coherences as there are spin interactions, and yields often overcrowded spectra.

On the other hand, one way to reduce the number of correlations that contribute to the structure of NMR spectra consists in using semi-selective pulses (low power r.f. fields).[25] These soft pulses allow handling coherences involving a single spin nucleus. In this latter case however, reducing the number of interactions that contribute to the multiplet structure of a given signal, without reducing the number of signals is almost impossible.

Finally, the combination of hard and soft pulses, and notably the implementation of refocusing blocks or filters, cannot get rid of this limitation.

The idea behind the gradient frequency encoding approach is to fully control the number of spin interactions that contribute to each correlation on an NMR spectrum, in order to (i) enhance resolution by limiting the line width, and (ii) make the analytical content of the spectrum more accessible (*i.e.* easily assignable *and* measurable).[26]

This methodology has given birth to powerful applications such as “pure shift” NMR[26-28], or more recently the Gradient encoded homonuclear SElective ReFocusing experiment (G-SERF). [29] A spatial frequency encoding is created along the sample, which allows to select, in separate cross sections, each spin-spin interaction that is involved in the coupling network around a given proton site. On the resulting 2D spectrum, each coupling can be straightforwardly assigned and measured, on a fully resolved multiplet, at the resonance frequency of the coupling partner.

The high resolution that is obtained on spectra recorded on a spatially frequency encoded sample, as well as the extreme simplicity of their analytical content, has changed this technique into a particularly promising tool. This spatial frequency encoding approach has been applied to the visualisation of enantiomers dissolved in a chiral liquid crystal: the complete set of ^{1}H-^{1}H residual dipolar couplings (RDC) could be measured and assigned for a model racemate, within an experimental time that was shorter than the one required by classical high resolution techniques.[30].

References

1 D. L. Rabenstein, J. Chem. Educ., **61**, 909-913, (1984)

2 P. Schanda, B. Brutscher, J. Am. Chem. Soc., **127**, 8014-8015, (2005)

3 P. Schanda, V. Forge, B. Brutscher, Proc. Natl. Acad. Sci. U. S. A., **104**, 11257-11262, (2007)

4 P. Schanda, E. Kupce, B. Brutscher, J. Biomol. NMR, **33**, 199-211, (2005)

5 R. M. Rasia, E. Lescop, J. F. Palatnik, J. Boisbouvier, B. Brutscher, J. Biomol. NMR, **51**, 369-378, (2011)

6 L. Frydman, T. Scherf, A. Lupulescu, Prog. NMR Spec., **99**, 15858-15862, (2002)

7 J. Jeener, in International Ampere Summer School, Basko Polje, Yugoslavia, 1971.

8 L. Frydman, A. Lupulescu, T. Scherf, J. Am. Chem. Soc., **125**, 9204-9217, (2003)

9 P. Pelupessy, J. Am. Chem. Soc., **125**, 12345-12350, (2003)

10 Y. Shrot, B. Shapira, L. Frydman, J. Magn. Reson., **171**, 163-170, (2004)

11 A. Tal, B. Shapira, L. Frydman, J. Magn. Reson., **176**, 107-114, (2005)

12 P. Giraudeau, S. Akoka, J. Magn. Reson., **186**, 352–357, (2007)

13 P. Giraudeau, Y. Shrot, L. Frydman, J. Am. Chem. Soc., **131**, 13902–13903, (2009)

14 M. Gal, P. Schanda, B. Brutscher, L. Frydman, J. Am. Chem. Soc., **129**, 1372-1377, (2007)

15 A. Herrera, E. Fernández-Valle, R. Martínez-Álvarez, D. Molero, Z. D. Pardo, E. Sáez, M. Gal, Angewandte Chemie-International Edition, **48**, 6274-6277, (2009)

16 M. Pathan, S. Akoka, I. Tea, B. Charrier, P. Giraudeau, Analyst, **136**, 3157-3163, (2011)

17 P. Giraudeau, S. Massou, Y. Robin, E. Cahoreau, J.-C. Portais, S. Akoka, Anal. Chem., **83**, 3112-3119, (2011)

18 A. Tal, L. Frydman, Prog. NMR Spec., **57**, 241–292, (2010)

19 T. C. Farrar, Anal. Chem., **42**, 109A-112A, (1970)

20 R. R. Ernst, G. Bodenhausen, A. Wokaun, in Principles of Nuclear Magnetic Resonance in One and Two Dimensions, Second ed., Clarendon Press, Oxford, 1987.

21 W. P. Aue, J. Karhan, R. R. Ernst, J. Chem. Phys., **64**, 4226-4227, (1976)

22 D. Marion, K. Wüthrich, Biochem. Biophy. Res. Com., **113**, 967-974, (1983)

23 M. Ottiger, F. Delaglio, A. Bax, J. Magn. Reson., **131**, 373-378, (1998)

24 B. L. Marquez, W. H. Gerwick, R. T. Williamson, Magn. Res. Chem., **39**, 499-530, (2001)

25 R. Freeman, Chemical Reviews, **91**, 1397-1412, (1991)

26 N. Giraud, M. Joos, J. Courtieu, D. Merlet, Magn. Res. Chem., **47**, 300-306, (2009)

27 K. Zangger, H. Sterk, J. Magn. Reson., **124**, 486-489, (1997)
28 G. Morris, J. Aguilar, R. Evans, S. Haiber, M. Nilsson, J. Am. Chem. Soc., **132**, 12770-12772, (2010)
29 N. Giraud, L. Beguin, J. Courtieu, D. Merlet, Angewandte Chemie-International Edition, **49**, 3481-3484, (2010)
30 D. Merlet, L. Beguin, J. Courtieu, N. Giraud, J. Magn. Reson., **209**, 315-322, (2011)

FAST NMR

Nicolas Giraud - NMR in Oriented Media Group

Quick Overview ...

... Fast Methods in NMR

• **FDM (Filter Diagonalisation Method)**	(Mandelshtam & Shaka)
• **Hadamard**	(Kupce & Freeman)
• **Red. Dimensionality:**	(Szyperski, Wüthrich, Brutscher,
GFT* / MWD- / APSY	(Gronenborn, Billeter, Markley, ...)
• **Projection Reconstruction**	(Kupce & Freeman)
• **Non-Linear Sampling**	(Wagner, Orekhov, Marion, ...)
• **Ultrafast 2D**	(Frydman, Pelupessy)
• **Covariance NMR**	(Brüschweiler, ...)
• **Spectrum Folding**	(Sidebottom, Berger, ...)
• **Sharc NMR**	(Sakhaii)
• **Rapid Pulsing**	(Ross, Pervushin, Brutscher,...)
• **Simultaneous Data Acquisition**	(Soerensen, Griesinger, Parella, ...)
• **gNMR**	(Giraud, Merlet,...)

from R. Weisemann, NMR Application Laboratories, Bruker Biospin Rheinstetten, DE

Quick Overview ...

... Fast Methods in NMR

• **FDM (Filter Diagonalisation Method)**	(Mandelshtam & Shaka)
• **Hadamard**	(Kupce & Freeman)
• **Red. Dimensionality:**	(Szyperski, Wüthrich, Brutscher,
GFT* / MWD- / APSY	(Gronenborn, Billeter, Markley, ...)
• **Projection Reconstruction**	(Kupce & Freeman)
• **Non-Linear Sampling**	(Wagner, Orekhov, Marion, ...)
• **Ultrafast 2D**	(Frydman, Pelupessy)
• **Covariance NMR**	(Brüschweiler, ...)
• **Spectrum Folding**	(Sidebottom, Berger, ...)
• **Sharc NMR**	(Sakhaii)
• **Rapid Pulsing**	(Ross, Pervushin, Brutscher,...)
• **Simultaneous Data Acquisition**	(Soerensen, Griesinger, Parella, ...)
• **gNMR**	(Giraud, Merlet,...)

from R. Weisemann, NMR Application Laboratories, Bruker Biospin Rheinstetten, DE

FAST NMR : why always faster ?!

Time Scales in NMR ...

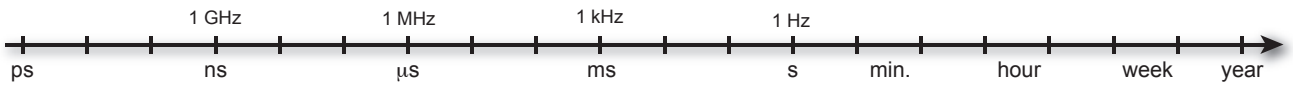

From A. Krushelnitsky, D. Reichert PNMR 47 (2005) 1–25

FAST NMR : why always faster ?!

Time Scales in NMR ...

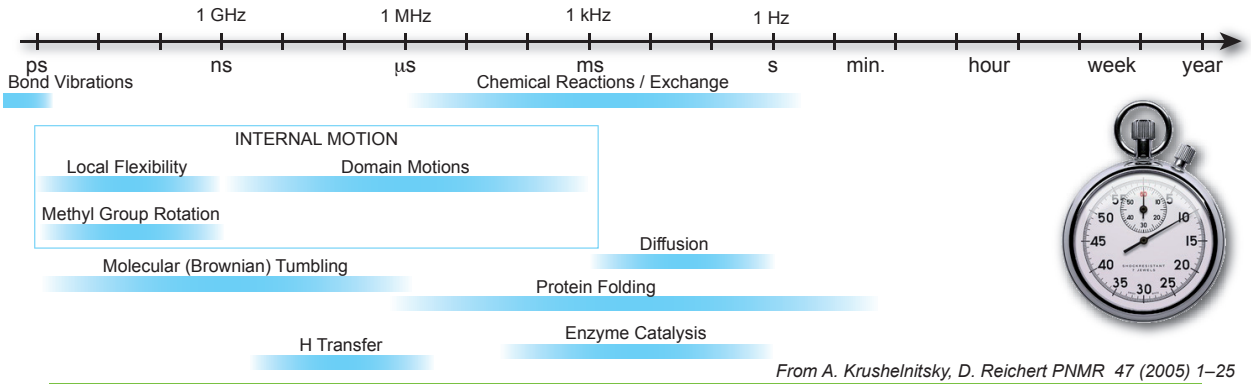

From A. Krushelnitsky, D. Reichert PNMR 47 (2005) 1–25

FAST NMR : why always faster ?!

Time Scales in NMR ...

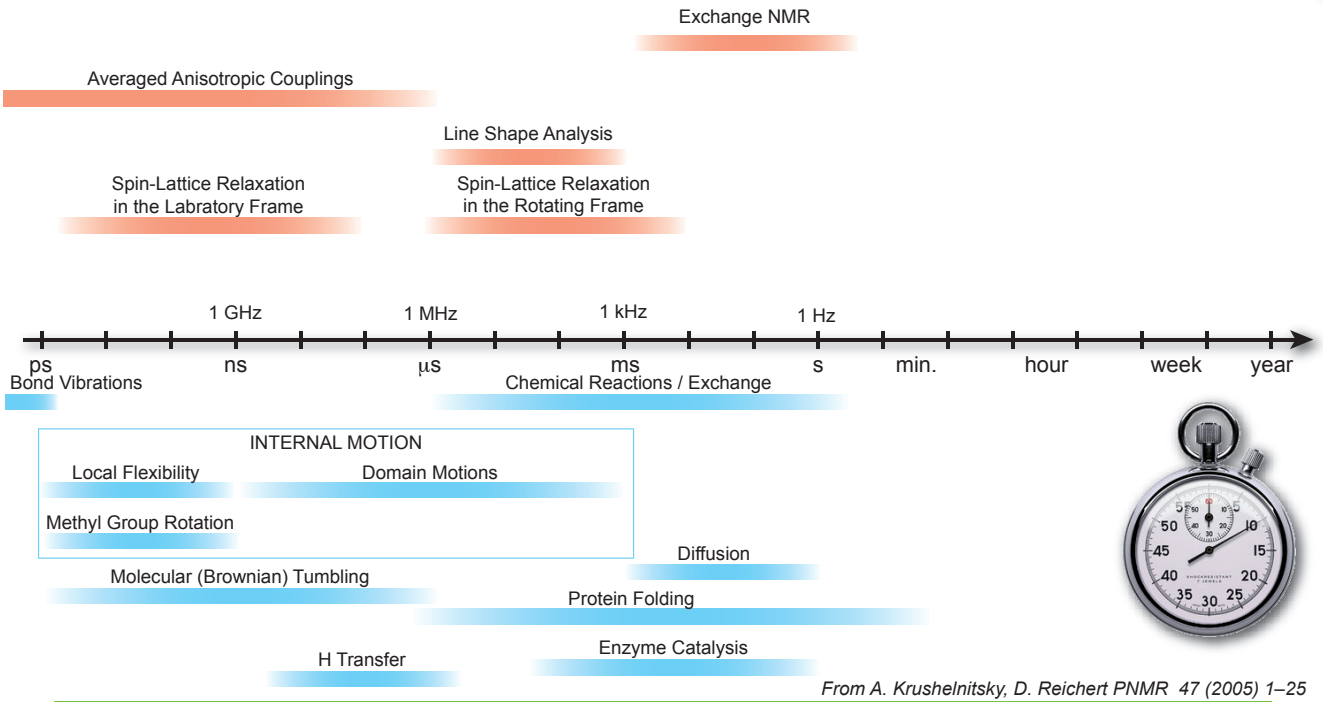

From A. Krushelnitsky, D. Reichert PNMR 47 (2005) 1–25

Experiment and Modelling in Structural NMR Advanced Concepts - *Fast NMR*

FAST NMR : why always faster ?!

Time Scales in NMR ...

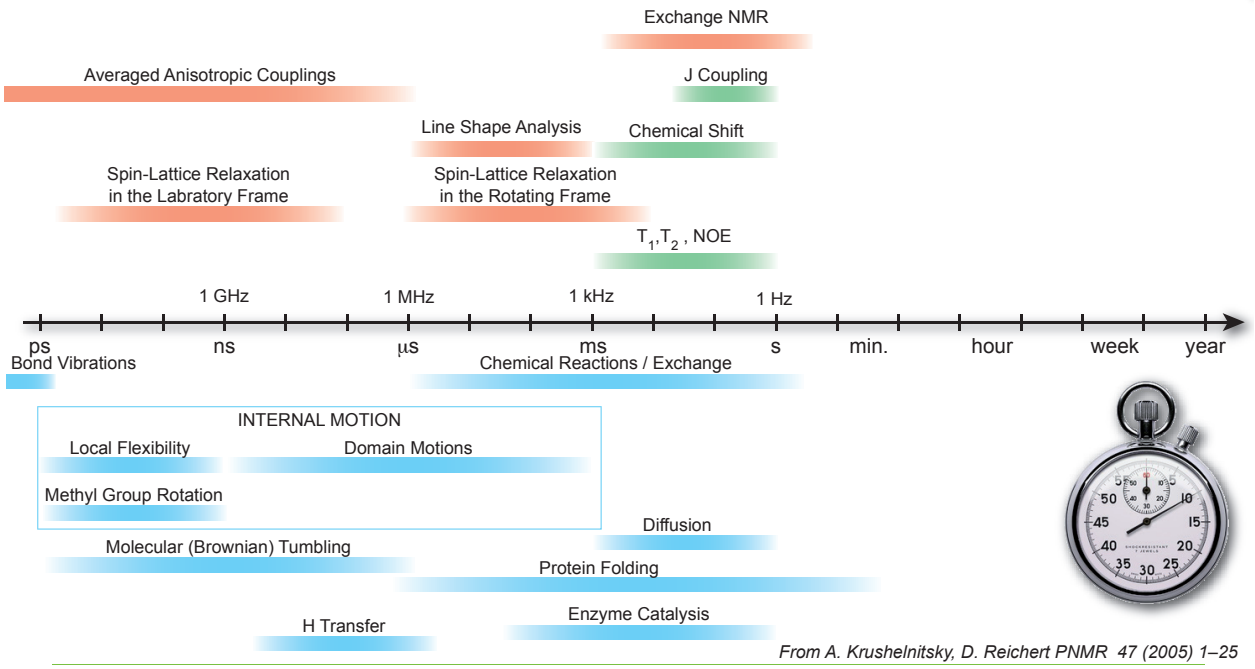

From A. Krushelnitsky, D. Reichert PNMR 47 (2005) 1–25

FAST NMR : why always faster ?!

Time Scales in NMR ...

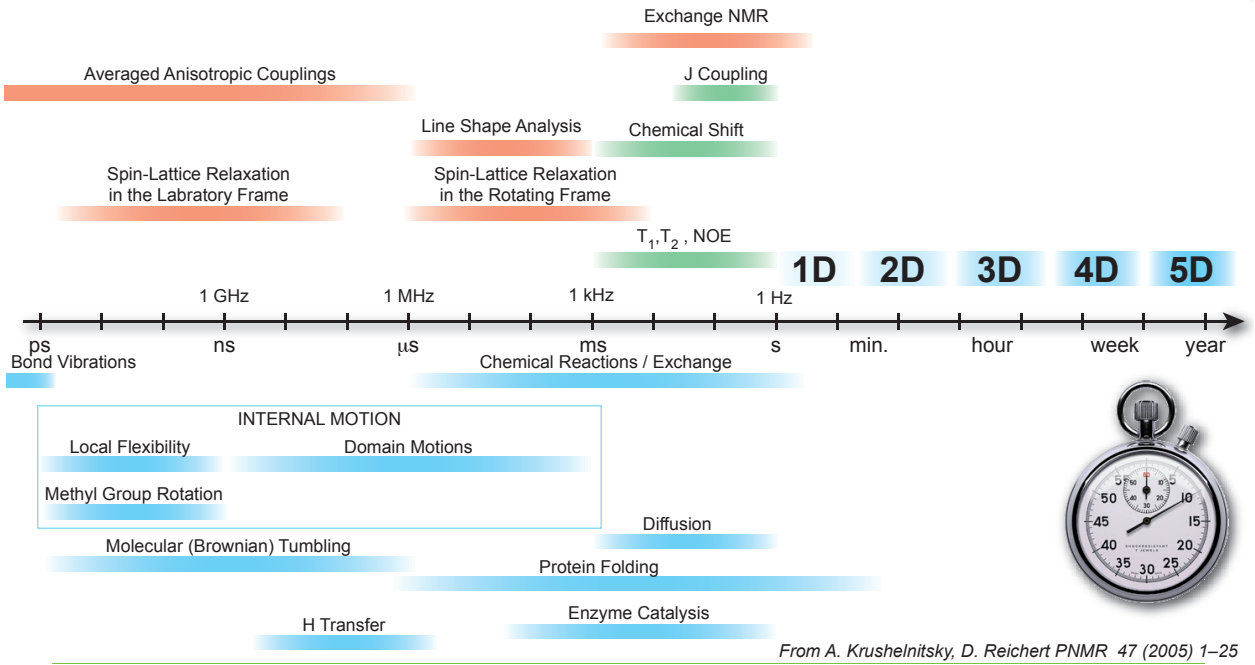

From A. Krushelnitsky, D. Reichert PNMR 47 (2005) 1–25

Experiment and Modelling in Structural NMR Advanced Concepts - *Fast NMR*

NMR: A Time Consuming Process ...
Delays in a Multidimensional Pulse Sequence

• Overall experimental time : $$D_{exp} \approx NS \cdot TD \cdot \left[D_1 + \frac{t_1^{max}}{2} + t_2 \right]$$

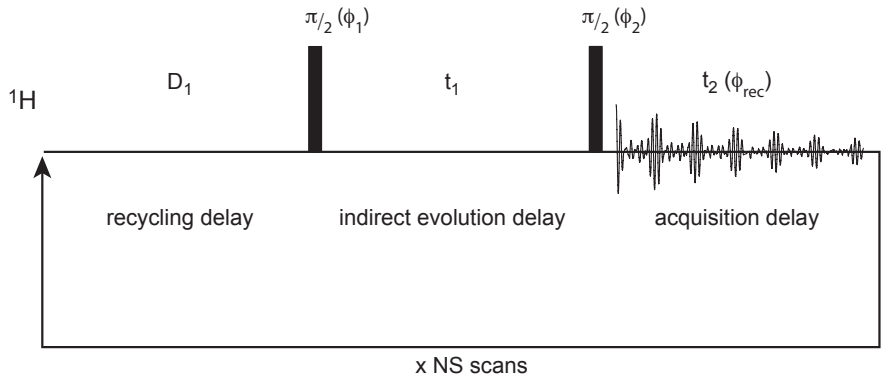

NMR: A Time Consuming Process ...
Delays in a Multidimensional Pulse Sequence

• Overall experimental time : $$D_{exp} \approx NS \cdot TD \cdot \left[D_1 + \frac{t_1^{max}}{2} + t_2 \right]$$

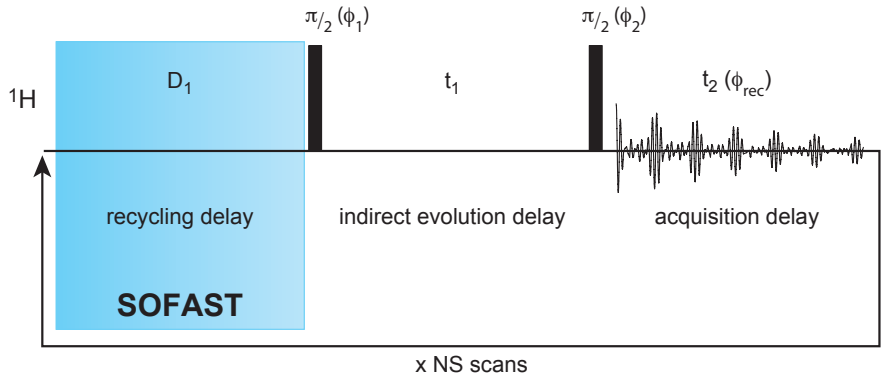

NMR: A Time Consuming Process ...
Delays in a Multidimensional Pulse Sequence

• Overall experimental time : $$D_{exp} \approx NS \cdot TD \cdot \left[D_1 + \frac{t_1^{max}}{2} + t_2 \right]$$

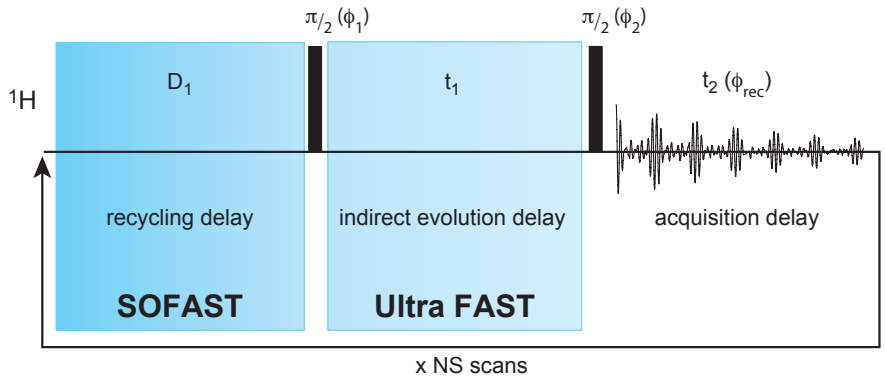

NMR: A Time Consuming Process ...
Overall Experimental & Analytical Process

The overall experimental and analytical process is limited by the high number of experiments required to:
• measure every relevant NMR probe of the structure and/or its dynamics
• extract their analytical content (assignment, measurement ...)

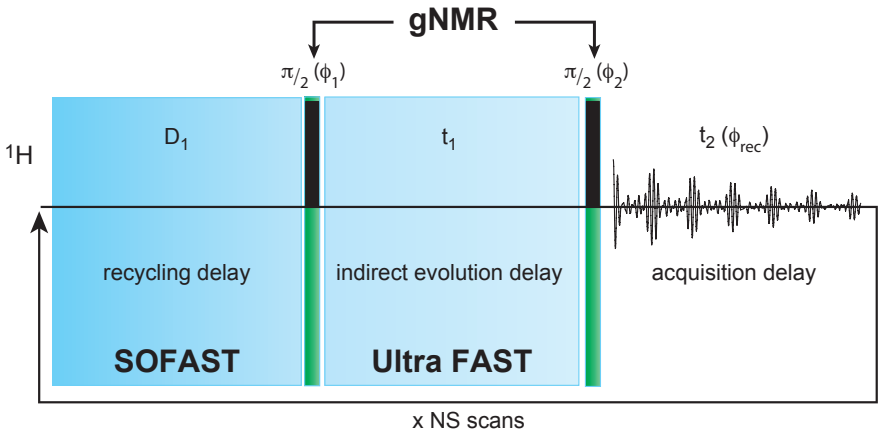

• This limitation is linked to intrinsic properties of irradiation schemes that are used to handle spin magnetization ...

band-Selective Optimized Flip-Angle Short-Transient

(SOFAST) Spectroscopy

Fast Data Acquisition : SOFAST Approach

Repetition Rate vs Longitudinal Relaxation

• Longitudinal relaxation is limiting the repetition rate for π/2 flip angles ...

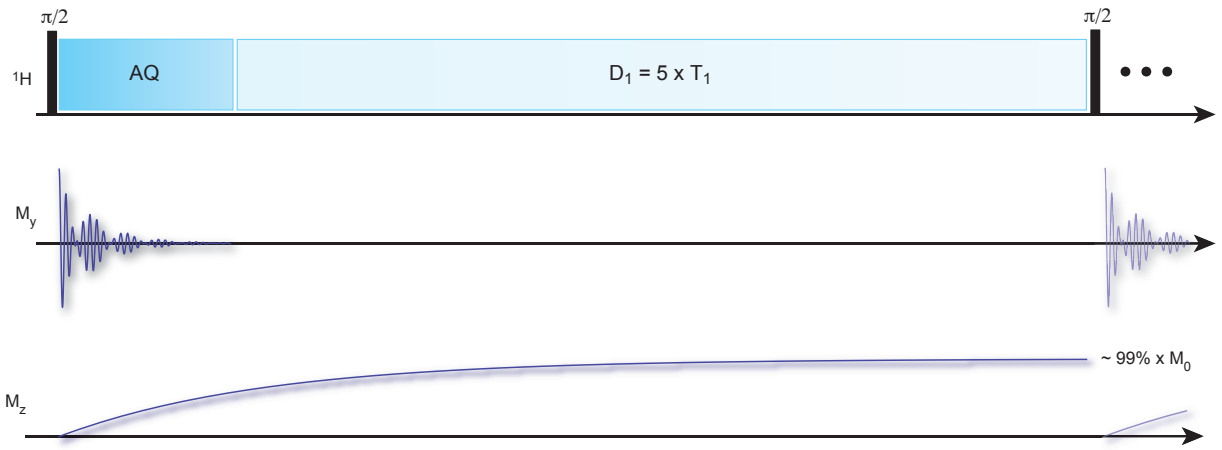

Fast Data Acquisition : SOFAST Approach

Euler Angle: Optimization of Sensitivity and Repetition Rate

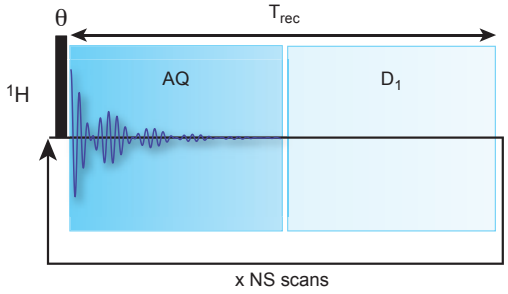

$$\cos(\theta_{Ernst}) = e^{-Trec / T_1}$$

$M_z = M_0.(1-\{1-\cos(\theta)\}.e^{-Trec/T_1})$

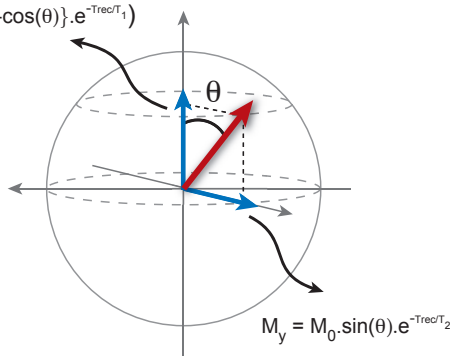

• For short T_{rec} , a maximum (non quantitative) sensitivity is obtained for the Ernst Angle

Fast Data Acquisition : SOFAST Approach

Euler Angle: Optimization of Sensitivity and Repetition Rate

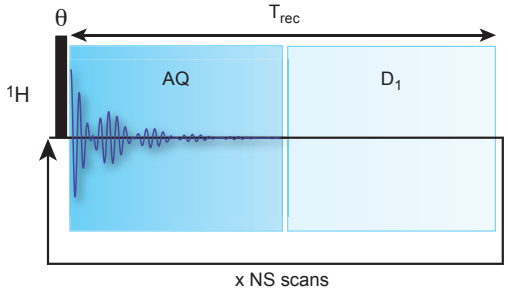

$$\frac{S}{N} \propto \frac{\left(1 - e^{-Trec/T_1}\right)\sin\theta}{1 - e^{-Trec/T_1}\cos\theta} M_0$$

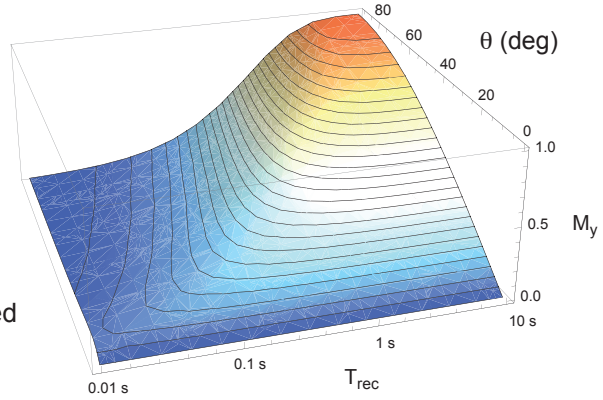

• The steady-state value of transverse magnetization after a pulse is a function of both the repetition time and the flip angle.

• Unfortunately, sensitivity is dramatically reduced when short transients need to be acquired ...

Fast Data Acquisition : SOFAST Approach

Longitudinal Relaxation Mechanisms in Macromolecules

For a given proton spin in a protein, additional sources of relaxation can influence the return to equilibrium of its longitudinal magnetization ...

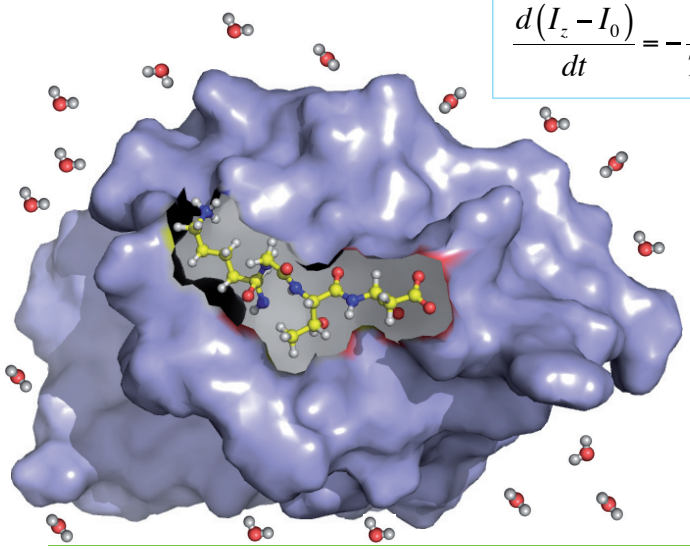

$$\frac{d(I_z - I_0)}{dt} = -\frac{1}{T_1}(I_z - I_0) - \sum_S \rho_{SI}(I_z - S_z) - \sum_S \sigma_{IS}(S_z - S_0)$$

- Pure longitudinal relaxation
- Cross-relaxation
- Spin diffusion
- Chemical exchange with water ...

Fast Data Acquisition : SOFAST Approach

Longitudinal Relaxation Mechanisms in Macromolecules

For macromolecules in solution, a longitudinal relaxation enhancement is observed, that leads to shorter apparent ^{1}H T_1's for amide protons when they are selectively excited.

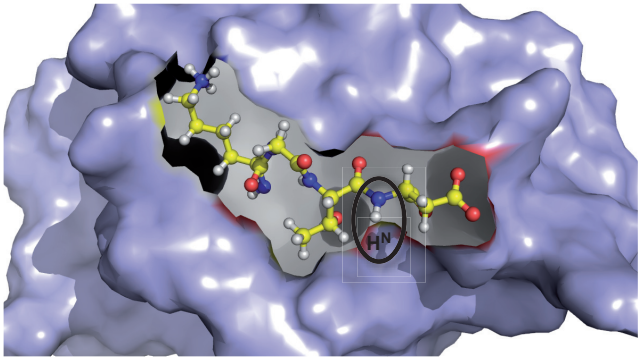

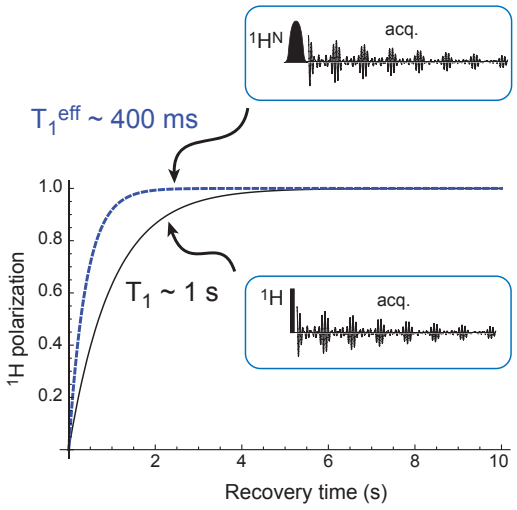

J|A|C|S COMMUNICATIONS

Published on Web 05/14/2005

Very Fast Two-Dimensional NMR Spectroscopy for Real-Time Investigation of Dynamic Events in Proteins on the Time Scale of Seconds

Paul Schanda and Bernhard Brutscher*

Institut de Biologie Structurale Jean-Pierre Ebel CNRS-CEA-UJF, 41 rue Jules Horowitz, 38027 Grenoble, France

Received March 2, 2005; E-mail: bernhard.brutscher@ibs.fr

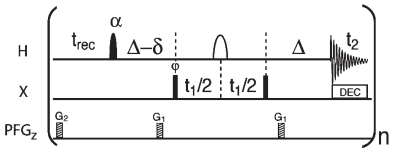

Figure 1. SOFAST-HMQC experiment to record ^{1}H- X (X) ^{15}N or ^{13}C) correlation spectra of proteins. Filled and open pulse symbols indicate 90° and 180° rf pulses, except for the first ^{1}H excitation pulse applied with flip angle R. The variable flip-angle pulse has a polychromatic PC9 shape,[8a] and band-selective ^{1}H refocusing is realized using an r-SNOB profile.[8b] The transfer delay Δ is set to $1/(2J_{HX})$, the delay δ accounts for spin evolution during the PC9 pulse, and t_{rec} is the recycle delay between scans. Adiabatic WURST-2 decoupling[8c] is applied on X during detection. Quadrature detection in t_1 is obtained by phase incrementation of φ according to TPPI-STATES.

Schanda, P. & Brutscher, B. JACS 127 (22), 8015 (2005)

J|A|C|S COMMUNICATIONS

Published on Web 05/14/2005

Very Fast Two-Dimensional NMR Spectroscopy for Real-Time Investigation of Dynamic Events in Proteins on the Time Scale of Seconds

Paul Schanda and Bernhard Brutscher*

Institut de Biologie Structurale Jean-Pierre Ebel CNRS-CEA-UJF, 41 rue Jules Horowitz, 38027 Grenoble, France

Received March 2, 2005; E-mail: bernhard.brutscher@ibs.fr

$$\left(\frac{S}{N}\right)_t \propto \frac{\left(1-e^{-T_{rec}/T_1}\right)\sin\beta}{\left(1-e^{-T_{rec}/T_1}\cos\beta\right)} \cdot \frac{1}{\sqrt{T_{scan}}}$$

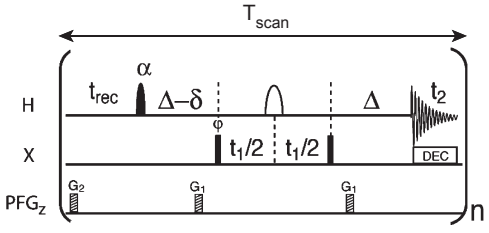

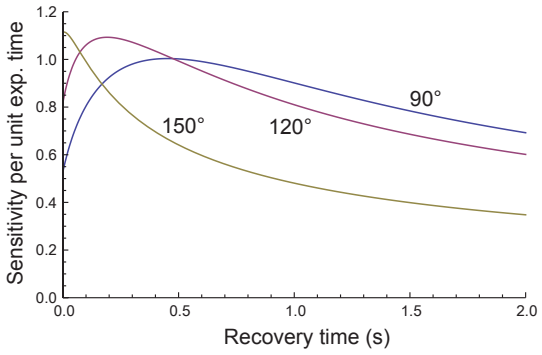

Schanda, P. & Brutscher, B. JACS 127 (22), 8015 (2005)

Experiment and Modelling in Structural NMR — Advanced Concepts - *Fast NMR*

J|A|C|S COMMUNICATIONS

Published on Web 05/14/2005

Very Fast Two-Dimensional NMR Spectroscopy for Real-Time Investigation of Dynamic Events in Proteins on the Time Scale of Seconds

Paul Schanda and Bernhard Brutscher*

Institut de Biologie Structurale Jean-Pierre Ebel CNRS-CEA-UJF, 41 rue Jules Horowitz, 38027 Grenoble, France

Received March 2, 2005; E-mail: bernhard.brutscher@ibs.fr

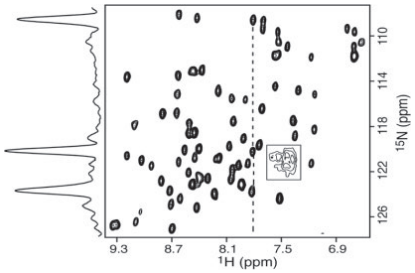

Figure 2. ^{1}H- ^{15}N correlation spectrum (central part) of ubiquitin (2 mM, pH 4.7) recorded at 800 MHz in only 5 s using the sequence of Figure 1. The acquisition parameters were set to: R) 120°, Δ) 5.4 ms, δ) 1.2 ms, t_2^{max}) 40 ms, and t_{rec}) 1 ms. Forty complex points (n) 80 + 4 dummy scans) were recorded for t_1^{max}) 22 ms. The band-selective ^{1}H pulses were centered at 8.0 ppm covering a bandwidth of 4.0 ppm. SOFAST-HMQC yields good water suppression in a single transient. The peak pattern surrounded by a box arises from Arg side chain resonances.

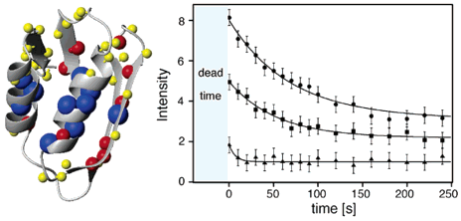

Figure 3. H/D exchange kinetics measured in the small protein MerAa (pH 7.5). On the right, the cross-peak intensities measured in a series of SOFAST-HMQC spectra are plotted as a function of exchange time for V25 (9), L53 (b), and A43 (2). A fit to the function $I(t)$) a_0 exp(- t/τ_{ex}) + a_1 yields exchange time constants τ_{ex}) 69 s for V25 and τ_{ex}) 53 s for L53. No reliable fit is possible for A43, but the upper limit can be estimated to τ_{ex} < 15 s. On the left, the measured exchange rates, divided in three classes (i) τ_{ex} < 15 s (yellow small spheres), (ii) 15 s < τ_{ex} < 40 s (red medium-size spheres), and (iii) τ_{ex} > 40 s (blue large spheres), are represented on the ribbon structure of MerAa.[5]

Protein folding and unfolding studied at atomic resolution by fast two-dimensional NMR spectroscopy

Paul Schanda*, Vincent Forge †, and Bernhard Brutscher* ‡

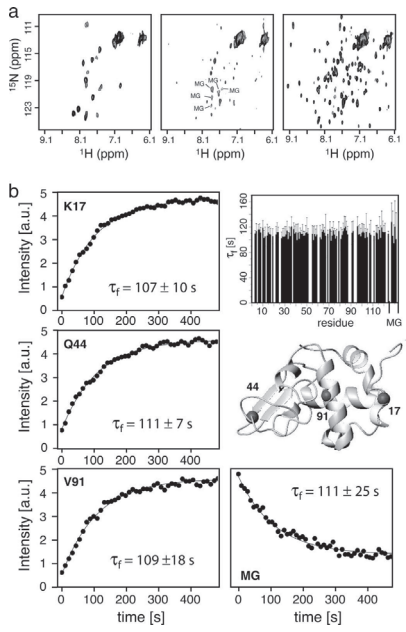

Fig. 2. Folding of α-lactalbumin studied by SOFAST real-time 2D NMR. (a) FTA-SOFAST-HMQC spectra of bovine α-lactalbumin at pH 2.0 (Left), immediately after a sudden pH jump to pH 8.0 that triggers folding (Center), and 120 s after injection (Right). Each spectrum shows the sum of two acquisitions of 10.9-s duration. Peaks corresponding to the MG state that disappear during folding are annotated. (b) Refolding kinetics of bovine α-lactalbumin from the MG state to the native state. The measured peak intensities are plotted as a function of the folding time. Shown are three residues situated in loop (K17), β-sheet (Q44), and α-helical regions (V91) that are indicated on the structure (Protein Data Bank ID code 1F6R). In addition, the signal decay observed for a peak assigned to the MG state is shown. Solid lines represent best fits to a three-parameter exponential function. A histogram shows the measured folding time constants for 92 residues in the native state as well as the 5 rates measured for the disappearance of the MG state.

www.pnas.org /cgi /doi /10.1073 /pnas.0702069104

PNAS | July 3, 2007 | vol. 104 | no. 27 | 11257–11262

Protein folding and unfolding studied at atomic resolution by fast two-dimensional NMR spectroscopy

Paul Schanda*, Vincent Forge †, and Bernhard Brutscher* ‡

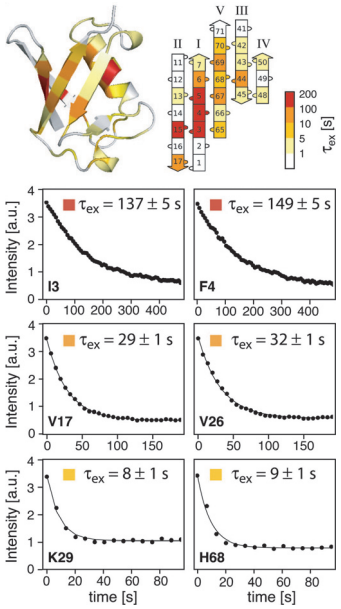

Fig. 3. H/D exchange data obtained for human ubiquitin at pH 11.95 by using SOFAST real-time 2D NMR. (Upper) The measured exchange rates are color-coded on the ubiquitin structure. (Lower) Examples of exchange curves corresponding to different exchange regimes together with the fitted exchange time constants. For residues color-coded in white, no signal decay was observed because the cross-peak intensity has decreased to its plateau value during the dead time of the experiment.

J Biomol NMR (2011) 51:369–378
DOI 10.1007/s10858-011-9567-4

ARTICLE

Rapid measurement of residual dipolar couplings for fast fold elucidation of proteins

Rodolfo M. Rasia · Ewen Lescop · Javier F. Palatnik
Jérôme Boisbouvier · Bernhard Brutscher

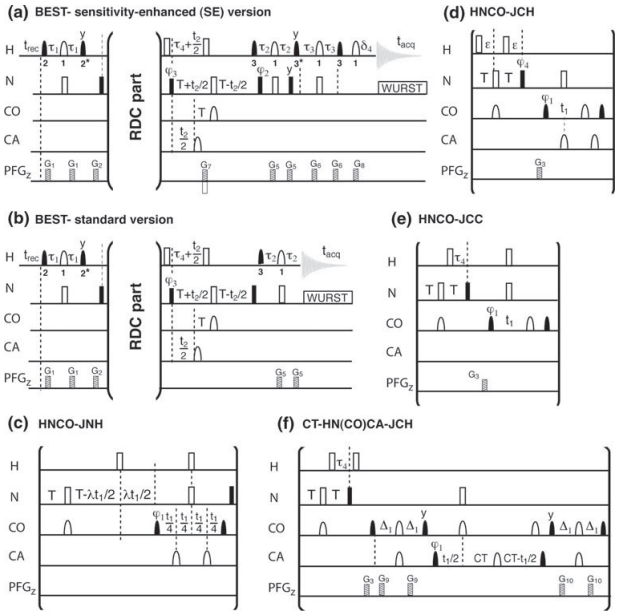

J Biomol NMR (2011) 51:369–378
DOI 10.1007/s10858-011-9567-4

ARTICLE

Rapid measurement of residual dipolar couplings for fast fold elucidation of proteins

Rodolfo M. Rasia · Ewen Lescop · Javier F. Palatnik
Jérôme Boisbouvier · Bernhard Brutscher

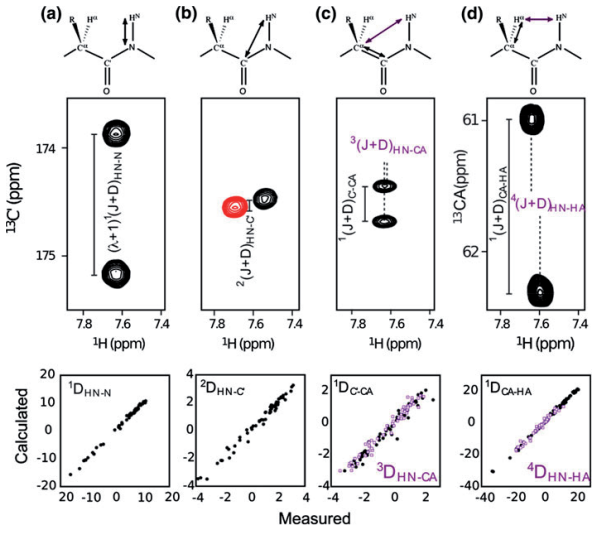

Fig. 2 Part of $^{1}H-^{13}C$ planes extracted from 3D data sets of BEST-HNCO-JNH (a), BEST HNCO-JCH (b), BEST HNCO-JCC (c), and BEST HN(CO)CA-JCH (d), showing cross-peak patterns of ubiquitin residue Gln62. The spin couplings that can be extracted from the different spectra are indicated ontop RDC correlation plots for each coupling measured on ubiquitin aligned in a bicelle medium are shown at thebottomof each spectrum [calculated RDC values are predicted from the high resolution solution structure of ubiquitin (PDB code : 1D3Z)] (Cornillescu et al. 1998)

J Biomol NMR (2011) 51:369–378
DOI 10.1007/s10858-011-9567-4

ARTICLE

Rapid measurement of residual dipolar couplings for fast fold elucidation of proteins

Rodolfo M. Rasia · Ewen Lescop · Javier F. Palatnik
Jérôme Boisbouvier · Bernhard Brutscher

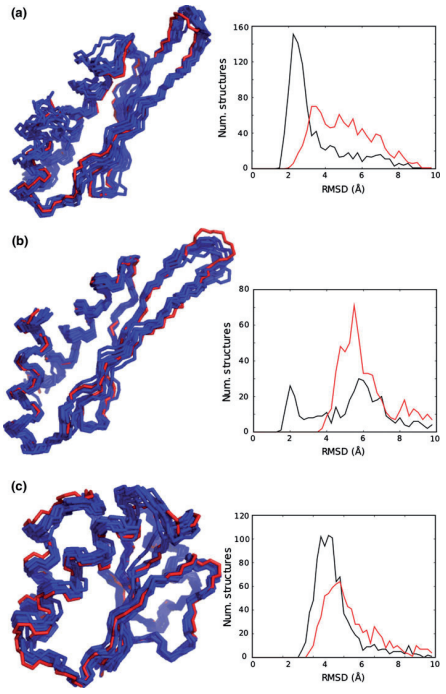

Fig. 4 Protein folds obtained using the present protocol. a HYL1-dsRBD1 b HYL1-dsRBD2 and c IIB-MTL. The ten lowest score structures (blue) are superimposed on the deposited crystal structure(red). The graph below shows the distribution of the RMSD of the calculated structures at the fragment insertion step either with (black) or without (red) RDC restraints, with respect to a reference structure

Experiment and Modelling in Structural NMR Advanced Concepts - *Fast NMR*

Ultra FAST (or Single Scan)

NMR Spectroscopy

Fast Data Acquisition : Ultra Fast NMR

Acquisition of a 2D experiment : classical approach

In a conventional 2D NMR experiment, the indirect domain is sampled over the acquisition of the same 1D experiment repeated N times, each time varying the evolution time t_1 ...

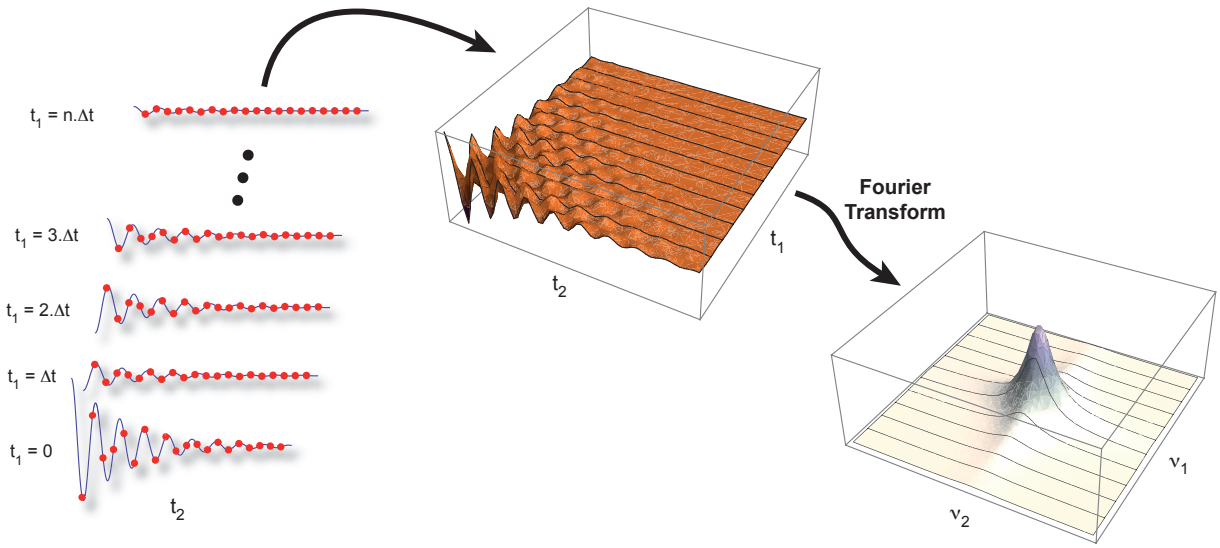

Fast Data Acquisition : Ultra Fast NMR

Acquisition of a 2D experiment : classical approach

In a conventional 2D NMR experiment, the indirect domain is sampled over the acquisition of the same 1D experiment repeated N times, each time varying the evolution time t_1 ...

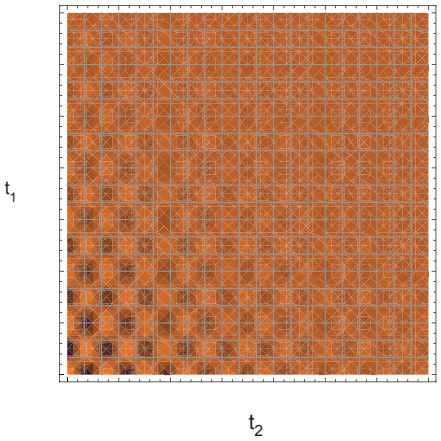

$$D_{exp} \approx NS \cdot TD \cdot \left[D_1 + \frac{t_1^{max}}{2} + t_2 \right]$$

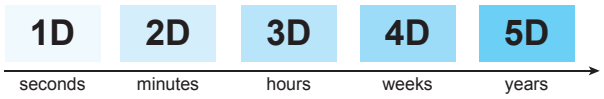

Fast Data Acquisition : Ultra Fast NMR

Acquisition of a 2D experiment : spatial time encoding

Frydman and coworkers have proposed to perform a parallel acquisition of the different sampled Δt_1 increments through a spatial time encoding of the NMR sample ...

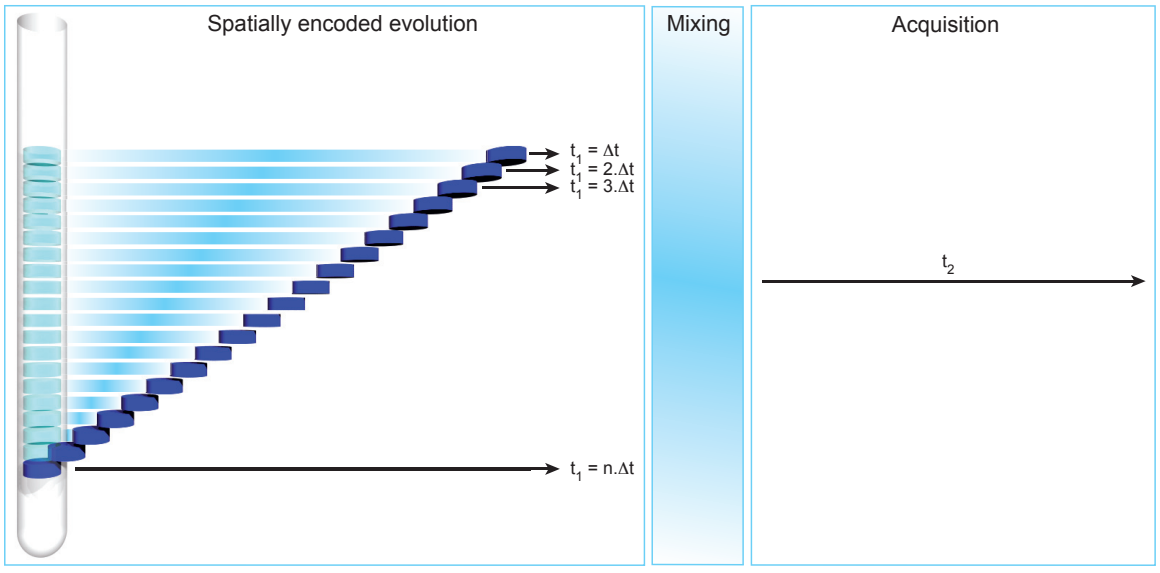

The acquisition of multidimensional NMR spectra within a single scan

Lucio Frydman [†‡], Tali Scherf [§], and Adonis Lupulescu [†]

Departments of [†]Chemical Physics and [§]Chemical Services, Weizmann Institute of Science, 76100 Rehovot, Israel

Communicated by Alexander Pines, University of California, Berkeley, CA, October 23, 2002 (received for review August 6, 2002)

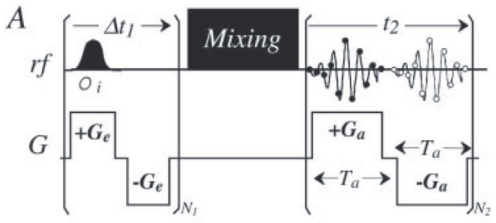

Fig. 3. (A) Generic scheme capable of affording 2D NMR spectra within a single scan. A train of frequency-shifted excitation pulses is applied in the presence of alternating field gradients to achieve an incremented evolution of spins throughout different positions in the sample (t_1); precession frequencies during the acquisition period then are monitored for each of these positions by using an EPI-type protocol (t_2). The nature of the mixing sequence is arbitrary. Throughout our experiments the B_o field heterogeneities were introduced along the main axis of a conventional sample tube by using the z gradients that are currently available in a majority of solution NMR systems.

The acquisition of multidimensional NMR spectra within a single scan

Lucio Frydman [†‡], Tali Scherf [§], and Adonis Lupulescu [†]

Departments of [†]Chemical Physics and [§]Chemical Services, Weizmann Institute of Science, 76100 Rehovot, Israel

Communicated by Alexander Pines, University of California, Berkeley, CA, October 23, 2002 (received for review August 6, 2002)

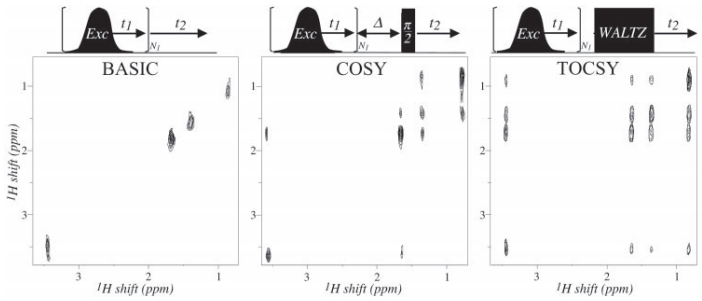

Fig. 4. Phase-sensitive single-scan 2D ^{1}H NMR spectra recorded within ≈0.22 s on a 20% (vol /vol) solution of n-butylchloride, $CH_3CH_2CH_2CH_2$-Cl, dissolved in $CDCl_3$. The pulse sequences used for acquiring these spectra are shown (Upper), with Δ set to 20 ms in the COSY and a 74-ms-long WALTZ sequence used for the TOCSY. Data were acquired with $N_1 = 40$ initial Gaussian pulses being applied at 4-kHz offset increments, while in the presence of $\gamma_H G_e = 150$ kHz /cm, and an acquisition involving 256 gradient echoes of the same magnitude with $T_a = 340$ μs long and 10-μs dwell times. All remaining pulses were applied nonselectively.

Experiment and Modelling in Structural NMR Advanced Concepts - *Fast NMR*

J|A|C|S
ARTICLES
Published on Web 07/04/2003

Principles and Features of Single-Scan Two-Dimensional NMR Spectroscopy

Lucio Frydman,*,† Adonis Lupulescu,† and Tali Scherf‡

$$S(k,t_2)=\int_z\int_{\nu_2}\int_{\nu_1}\left[P(z,\nu_1,\nu_2)e^{i\nu_1 t_1(z)}e^{i\nu_2 t_2}e^{ikz}\right]d\nu_1 d\nu_2 dz$$

$$S(k,t_2)=\rho\int_{\nu_2}\int_{\nu_1} I(\nu_1,\nu_2)e^{i\nu_1 t_1(z)}e^{i\nu_2 t_2}d\nu_1 d\nu_2$$

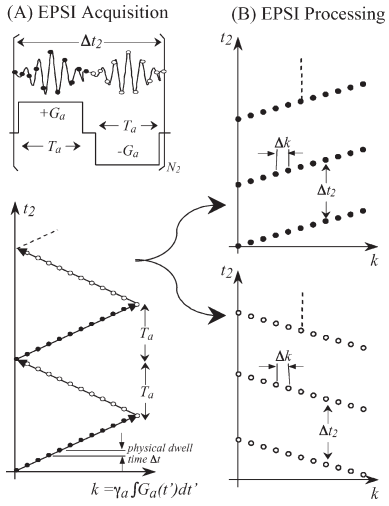

Figure 4. (A) Basics of the echo-planar spectroscopic imaging (EPSI) protocol employed throughout the present work to detect the spins' frequencies in a spatially resolved fashion. Signals are monitored as a function of k and t_2 variables; O and b dots symbolize the coordinates of points digitized during the course of positive and negative acquisition gradients. Such a gradient echo module is then repeated N_2 times, with N_2 defining the number of effective points along t_2. (B) As data stemming from an EPSI scheme employing a constant rate of digitization are not arrayed within a regular grid ready to be 2D FT, points need to be sorted out into two independent bidimensional data sets that are then individually processed. Both 2D data sets can then be co-added for the sake of improving the overall S/N.

J|A|C|S
ARTICLES
Published on Web 07/04/2003

Principles and Features of Single-Scan Two-Dimensional NMR Spectroscopy

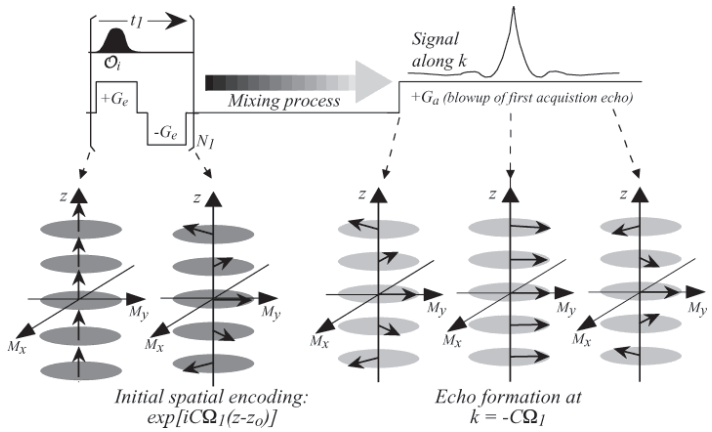

Figure 5. Simplified cartoon describing the origin of peaks along the indirect dimension of ultrafast 2D NMR experiments. The heterogeneous nature of the t_1 evolution leads to an encoding of the internal precession frequency Ω_1 along the z axis (second panel from left); this spiral of spin-packets is subsequently unwound by an acquisition gradient G_a possessing an identical z spatial dependence. The coherent addition of spin-packets thus leads to a sharp echo along the k coordinate whose position reveals the extent of Ω_1 encoding prior to the mixing processs in essence, the spectrum along the indirect dimension. Such "peak" formation is only illustrated here for a portion of the first acquisition gradient echo; the phase encoding gained by this echo peak during the course of the N_2 gradient-reversals occurring as a function of t_2 provides a conventional route to measure the Ω_2 frequencies active during the acquisition.

Experiment and Modelling in Structural NMR Advanced Concepts - *Fast NMR*

J|A|C|S
ARTICLES
Published on Web 07/04/2003

Principles and Features of Single-Scan Two-Dimensional NMR Spectroscopy

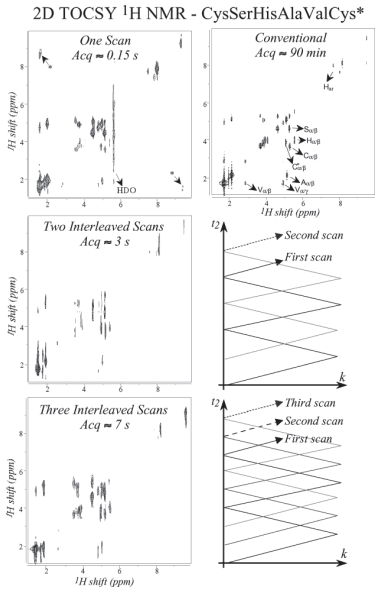

Figure 8. Acquisition strategies capable of easing the gradient demands of ultrafast NMR, based on extending the single-transient 2D experiment to a small number of interleaved scans spanning the *k*-space trajectories illustrated to the right of each spectrum. 2D TOCSY spectroscopy (50 ms WALTZ mixing, magnitude plotting) was chosen to illustrate these acquisition modes, using a solution of the indicated hexapeptide dissolved in D_2O (whose residual water resonance was largely eliminated using a 1.5 s presaturation pulse). Acquisition parameters for the various ultrafast experiments included N_1) 61, N_k) 66, N_2) 256, ΔO) 12 kHz, $\gamma_k G_c$) 300 kHz/cm, $\gamma_k G_a$) 300 kHz/cm, 1 μs dwell times, and 80 μs Gaussian excitation pulses for the single-scan acquisition; N_1) 23, N_k) 23, N_2) 256, ΔO) 8 kHz, $\gamma_k G_c$) 110 kHz/cm, $\gamma_k G_a$) 97 kHz/cm, 8 μs dwell times, and 100 μs Gaussian excitation pulses for the two-scan acquisition; N_1) 35, N_k) 35, N_2) 256, ΔO) 8 kHz, $\gamma_k G_c$) 180 kHz/cm, $\gamma_k G_a$) 90 kHz/cm, 8 μs dwell times, and 100 μs Gaussian excitation pulses for the three-scan acquisition. Most remaining experimental conditions were as in Figure 7. The differing ν_1 resolution observed among the various spectra is a consequence of the different number of N_1 slices chosen to carry out the acquisitions, and not of the increasing number of scans that were used. Asterisks in the single-scan acquisition indicate peaks arising from the "ghosting" phenomena further described in the text. A conventional 2D NMR spectrum showing a tentative assignment of the resonances is also illustrated for completion on the top-right panel.

UNIVERSITÉ PARIS SUD
Comprendre le monde, construire l'avenir®

J|A|C|S
ARTICLES
Published on Web 07/04/2003

Principles and Features of Single-Scan Two-Dimensional NMR Spectroscopy

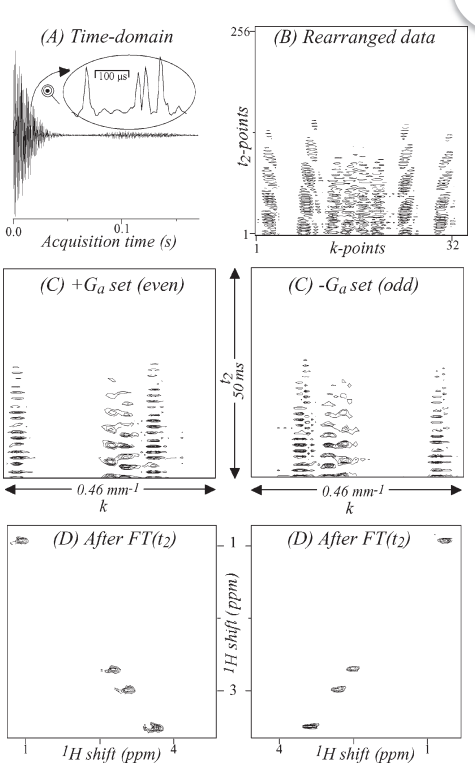

Figure 6. Summary of events involved in the single-scan acquisition of phase-sensitive 2D NMR spectra, illustrated with ^{1}H data recorded on a solution of *n*-butyl chloride dissolved in $CDCl_3$ and utilizing a 2D NMR sequence devoid from the actual mixing process. (A) Time-domain data collected using the spatially selective excitation/detection procedures illustrated in Figures 3 and 4; the magnified inset shows the signal (magnitude) arising from an individual T_a period, depicting in essence the compound's unidimensional ν_1 spectrum. (B) 2D contour plot of the unidimensional data set illustrated in (A), following a rearrangement of its $2N_kN_2$ points according to their *k* and t_2 coordinates. Interleaved data sets acquired with $+G_a$ and $-G_a$ gradients are still present at this point, thus resulting in a mirror-imaging of the signal along the *k*-axis. (C) Pairs of data sets resulting upon separating the interleaved $+G_a$/$-G_a$ arrays in (B) into two (k,t_2) signals possessing N_kN_2 points each. The signals shown in these sets have been subject to a phase correction and to a minor shearing that compensates for nonidealities in the acquisition gradient strengths (see below). Notice the spectral structure observed already at this point along the *k*-axis. (D) Mirror-imaged 2D NMR spectra arising upon subjecting the data sets in (C) to t_2 Fourier transformation.

J. AM. CHEM. SOC. 9 VOL. 125, NO. 30, 2003 **9210**

Experiment and Modelling in Structural NMR Advanced Concepts - *Fast NMR*

J|A|C|S
ARTICLES
Published on Web 09/13/2003

Adiabatic Single Scan Two-Dimensional NMR Spectrocopy

Philippe Pelupessy*,†

Contribution from the Département de Chimie, associé au CNRS, Ecole Normale Supérieure, 24 rue Lhomond, 75231 Paris Cedex 05, France

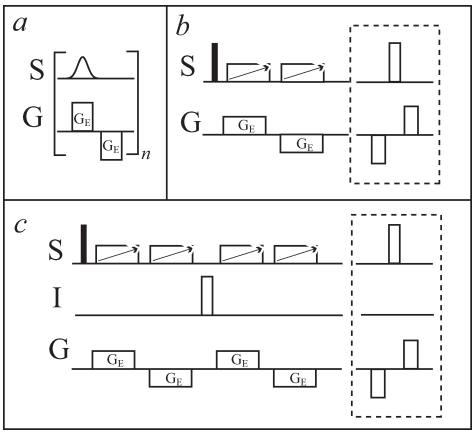

Figure 1. (a) Original excitation scheme proposed by Frydman et al.[3] to obtain the frequency labeling in the indirect ω_1 dimension in Frydman-Scherf-Lupulescu experiments (FSL experiments). A train of bipolar gradients and frequency selective pulses, the carrier frequency of which is stepped from the minimum to the maximum frequency that is induce by the gradients $\boldsymbol{G_E}$, is applied. This causes the evolution time t_1 of the spins $\boldsymbol{S}$ to depend on the sample position. (b) Excitation scheme for modified adiabatic FSL-experiments based on the use of frequency swept pulses during a constant time evolution period. After a nonselective $\pi/2$ pulse, a bipolar gradient pair is applied, while a frequency modulated adiabatic pulse is present during each gradient. In this scheme, the whole sample contributes to the signal and off-resonance effects of the pulses do not deteriorate the excitation profile. Heteronuclear decoupling can be introduced as shown in (c) by repeating the scheme twice, with a π pulse on the **I**-spins in between. The π pulse does not affect the chemical shift evolution of the **S**-spins but inverts the effect of the heteronuclear scalar coupling J_{IS}. The extra blocks in gray can be appended to shift the refocusing of the middle of the chemical shift range of the **S**-spins to the middle of the gradients applied during detection.

J|A|C|S
ARTICLES
Published on Web 09/13/2003

Adiabatic Single Scan Two-Dimensional NMR Spectrocopy

Philippe Pelupessy*,†

Contribution from the Département de Chimie, associé au CNRS, Ecole Normale Supérieure, 24 rue Lhomond, 75231 Paris Cedex 05, France

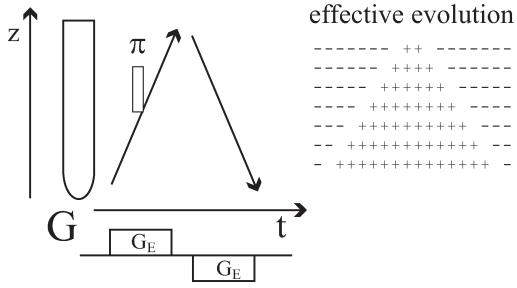

Figure 2. The effect of the two adiabatic pulses in the scheme of Figure 1b can be represented by two instantaneous π pulses that occur when the frequency of the adiabatic sweep passes through the resonance frequency of the spins.[10] Hence the spins near the bottom of the sample are refocused first while the ones at the top are affected last. For the second pulse the situation is time-reversed since the sign of the gradient is inverted. This results in differential evolution throughout the sample, as shown on the right of the figure.

J. AM. CHEM. SOC. 2003, *125*, 12345- 12350 **12345**

Experiment and Modelling in Structural NMR Advanced Concepts - *Fast NMR*

Available online at www.sciencedirect.com
SCIENCE DIRECT®
Journal of Magnetic Resonance 171 (2004) 163–170
JMR Journal of Magnetic Resonance
www.elsevier.com/locate/jmr

Communication

Ultrafast 2D NMR spectroscopy using a continuous spatial encoding of the spin interactions

Yoav Shrot, Boaz Shapira, Lucio Frydman *

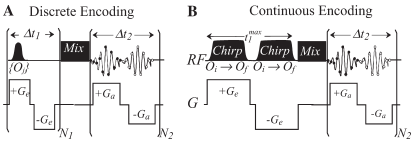

Fig. 1. Comparison betweentwo schemes capable of creating the kind of spatially encoded spin states demanded for the execution of amplitude-modulated 2D NMR spectroscopy within a single scan. (A) Original protocol whereby indirect-domain X_1 interactions are encoded by a discrete train of N_1 RF pulses, applied at constant frequency increments DO and spaced by constant delays Dt_1. Each excitation pulse is applied in combination with its own $\pm G_e$ excitation gradient echo; following the mixing process interactions are decoded using an oscillatory $\pm G_a$ acquisition gradient. (B) New scheme discussed in this work whereby the train of excitation pulses/gradient echoes in scheme (A) is replaced by a pair of continuous irradiation pulses in combination with a single bipolar gradient. Although both RF pulses are here identical the purpose of the first of these RF sweeps is to sequentially excite spins throughout the sample, whilst the purpose of the second one is to store the t_1-encoded coherences. See the text for additional details.

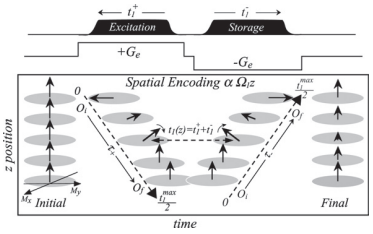

Fig. 2. Simplified description of the effects introduced by pre-mixing events in the pulse sequenceshown in Fig. 1B, on the spins' evolution. RF offsets O are assumed swept betweenan initial value O_i and a final value $O_f = -O_i$ at a constant rate R during both the "excitation" ($+G_e$) and the "storage" ($-G_e$) portions of the sequence For either the excitation or storage sweeps the RF will nutate by 90° spins whose z positions fulfill the $O(s_\pm) = O_i + R s_\pm = \pm c_e G_e z$ condition, as illustrated for the center spin-packet. The evolution time t_1^0 undergone by spin coherences during the course of the excitation sweepbecomesthen identical to the t_1^- free evolution period experienced over the storage sweep, for every z coordinate in the sample. This results in an $X_1 z$ dependence for the amplitude-modulated spin states stored at the conclusion of the sequence

J. AM. CHEM. SOC. 2003, *125*, 12345- 12350

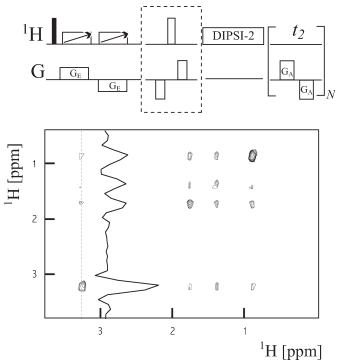

Figure 3. Scheme of Figure 1b followed by a TOCSY mixing sequence and the EPI-detection block. The experiment has been applied to a sample of 10% (vol/vol) *n*-butylbromide in $CDCl_3$.

Journal of Magnetic Resonance 171 (2004) 163–170

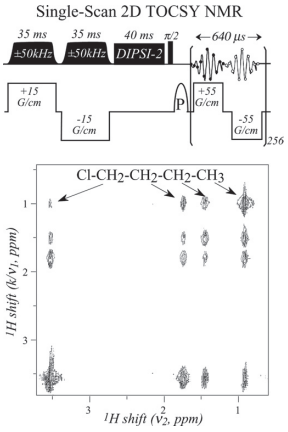

Fig. 3. Single-scan 2D TOCSY NMR spectrum acquired on an n-butylchloride/$CDCl_3$ sample, utilizing a sequence like the one illustrated on Fig. 1B with the following parameters: $G_e = 15$ G/cm, $O_i = -O_f = 50$ kHz, $t_1^{max} = 70$ ms, $G_a = 55$ G/cm, $N_2 = 256$, $T_a = 0.31$ ms sampled with a constant dwell of 2 ls, and a ±210 kHz filter bandwidth (derived from $\pm c_a G_a L/2$; L being the sample length). All gradient-switching times were set to 10 ls, and a 100 ls purging gradient pulse (P) was applied just prior to beginning data digitization in order to clean up undesired residual signals. The frequency-chirped RF pulses involved in this sequence were programmed in real time using the Pbox Varian software package, with a WURST-50 amplitude-modulated pulse shape, an adiabaticity parameter a ≈ 0.068, and a 2 ls digital resolution. A 40 ms long DIPSI-2 type sequence, applied in the absence of gradients and over a 10 kHz bandwidth, was employed for the mixing. The acquired data points were separated for their off-line processing into $+G_a$ and $-G_a$ contributions [10]; the contour plot illustrated in (B) then resulted from subjecting one of these sets to a suitable shearing, zero-filling to 256 · 512 (k, t_2)-points, Fourier transformation against t_2, and magnitude mode calculation.

Available online at www.sciencedirect.com
SCIENCE DIRECT®
Journal of Magnetic Resonance 176 (2005) 107–114
JMR Journal of Magnetic Resonance
www.elsevier.com/locate/jmr

Communication

A continuous phase-modulated approach to spatial encoding in ultrafast 2D NMR spectroscopy

Assaf Tal, Boaz Shapira, Lucio Frydman *

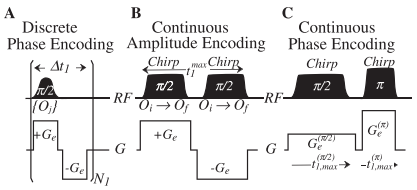

Fig. 1. Schemes capable of affording the spatial encoding pattern required for ultrafast 2D NMR acquisitions. (A) Discrete phase-modulated encoding protocol composed of a train of N_1RF pulses, applied at constant frequency increments $DO = (c_e G_e L)/(N_1 - 1)$ in combination with multiple $\pm G_e$ gradient oscillations. (B) Continuous amplitude-modulated scheme where a pair of identical frequency-swept irradiation pulses is applied over a range $\approx c_e G_e L$ in combination with a single bipolar gradient, to achieve the storage of a $\cos(CX_1z)$ longitudinal magnetization pattern. (C) New encoding scheme proposed in the present study, capable of yielding a phase-modulated $\exp(iCX_1z)$ transverse evolution without requiring the application of rapidly oscillating $\pm G_e$ gradients. Schemes are illustrated for a single-channel excitation for the sake of simplicity; see the text for further definitions.

One example of limitation of amplitude-modulated sequences: transfering of x and y components of magnetization in a transfer from I to S spin:

Phase-Modulation Amplitude-Modulation

$$\begin{cases} I_x \rightarrow S_x \\ I_y \rightarrow S_y \end{cases} \Leftrightarrow I_\alpha \rightarrow S_\alpha$$

Available online at www.sciencedirect.com
SCIENCE DIRECT®
Journal of Magnetic Resonance 176 (2005) 107–114
JMR Journal of Magnetic Resonance
www.elsevier.com/locate/jmr

Communication

A continuous phase-modulated approach to spatial encoding in ultrafast 2D NMR spectroscopy

Assaf Tal, Boaz Shapira, Lucio Frydman *

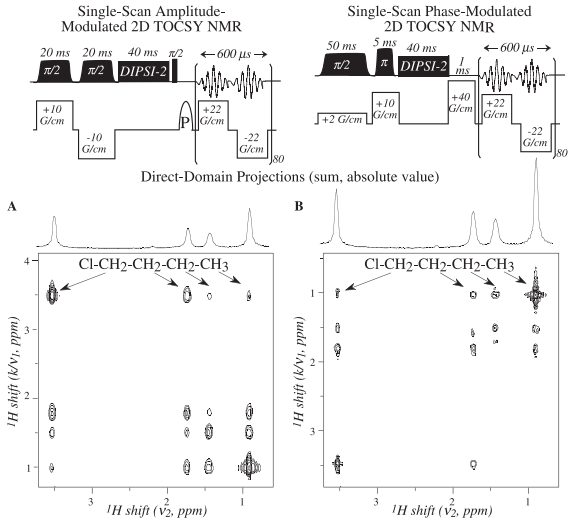

Available online at www.sciencedirect.com
ScienceDirect
Journal of Magnetic Resonance 186 (2007) 352–357
JMR Journal of Magnetic Resonance
www.elsevier.com/locate/jmr

Communication

A new detection scheme for ultrafast 2D J-resolved spectroscopy

Patrick Giraudeau *, Serge Akoka

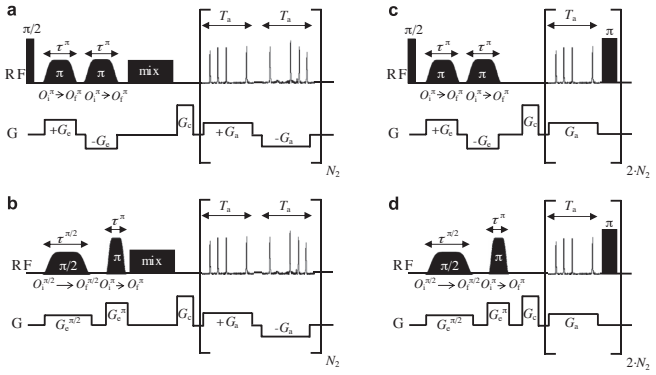

Fig. 1. (a and b) Pulse sequences for the acquisition of ultrafast 2D spectra, with phase-modulated encoding schemes proposed by Pelupessy (a) and Tal et al. (b), followed by the usual EPI detection block. (c and d) New ultrafast J-resolved detection scheme preceded by phase-modulated encoding schemes proposed by Pelupessy (c) and Tal et al. (d). The G_c gradient prior to acquisition is adjusted to set the middle of the chemical shift range in the middle of the detection period T_a. The 180° pulse phase is alternated as described in the text. Note that the detection loop is repeated $2N_2$ times in the new scheme to obtain the same number of FIDs than with the original EPI scheme.

Available online at www.sciencedirect.com
ScienceDirect
Journal of Magnetic Resonance 186 (2007) 352–357
JMR Journal of Magnetic Resonance
www.elsevier.com/locate/jmr

Communication

A new detection scheme for ultrafast 2D J-resolved spectroscopy

Patrick Giraudeau *, Serge Akoka

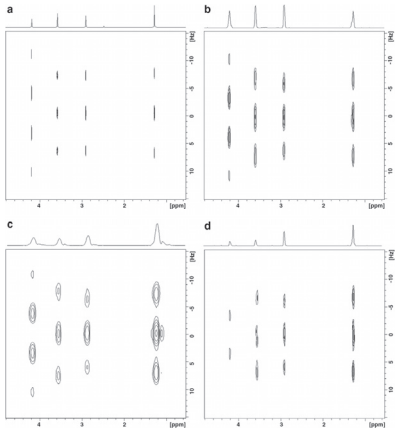

Fig. 3. Comparison between 500 MHz J-resolved spectra acquired on a 100 mmol L^{-1} 3-ethyl bromopropionate sample in $CDCl_3$ at 298 K. (a) Conventional spectrum acquired in 3 h 8 min with 32 t_1 increments and 16 scans. (b) Ultrafast spectrum obtained in 500 ms using Pelupessy's (b) or Tal's (c) phase-encoded excitation scheme followed by our new detection block. (d) Ultrafast spectrum acquired in 550 ms by combining the phase-encoded excitation schemes proposed by Tal and Pelupessy and the J-resolved detection block. All spectra, presented in magnitude mode, were processed with the same apodization function and post-processing parameters, as described in Section 4. For the mixed encoding scheme (d), the two external peaks of the quadruplet at 4.16 ppm are not visible for signal-to-noise reasons but can be observed on the corresponding column (Fig. 4 d).

Experiment and Modelling in Structural NMR Advanced Concepts - *Fast NMR*

Research Article

Magnetic Resonance in Chemistry

Received: 28 October 2008 Revised: 15 December 2008 Accepted: 18 December 2008 Published online in Wiley Interscience: 24 February 2009

(www.interscience.com) DOI 10.1002/mrc.2403

New developments in the spatial encoding of spin interactions for single-scan 2D NMR‡

Yoav Shrot,† Assaf Tal† and Lucio Frydman

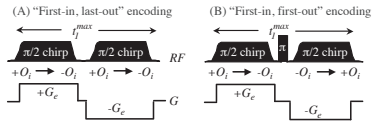

Figure 1. Comparison between (A) the original amplitude-modulated scheme yielding a 'first-in, last-out' linear spatial encoding (12) and (B) the new 'first-in, first-out' scheme discussed in this work, whereby spins at all positions spend equal times precessing in the transverse plane (and thereby are affected to the same extent by the T_2 decay) yet a linear $C\Omega_1 z$

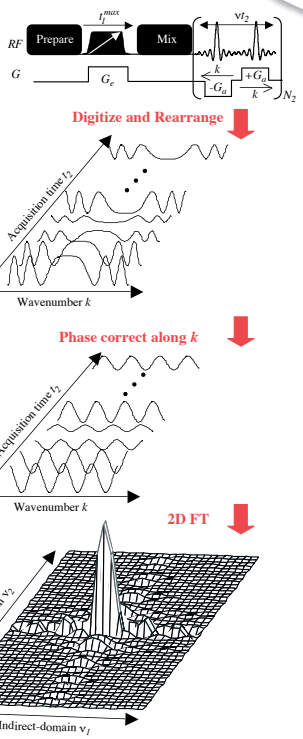

Figure 3. Top: new encoding scheme proposed for the execution of single-scan 2D NMR, based on the use of a single encoding-gradient/RF-pulse module. Bottom: various stages of data manipulation involved in the retrieval of the single-scan 2D spectrum including removal of the second-degree k dependence and 2D FT of the resulting $S(k, t_2)$ data, as described in the text.

Research Article

Magnetic Resonance in Chemistry

Received: 28 October 2008 Revised: 15 December 2008 Accepted: 18 December 2008 Published online in Wiley Interscience: 24 February 2009

(www.interscience.com) DOI 10.1002/mrc.2403

New developments in the spatial encoding of spin interactions for single-scan 2D NMR‡

Yoav Shrot,† Assaf Tal† and Lucio Frydman

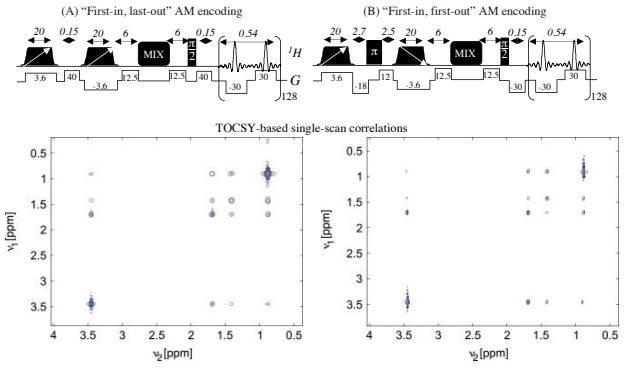

Figure 2. Outcomes observed upon applying the single-scan 2D NMR principles introduced in Fig. 1, to an *n*-butylchloride/$CDCl_3$ sample. Shown on top are the traditional (left) and newly proposed (right) encoding sequences used in these tests, with gradients and timing parameters (in G/cm and ms) indicated. White arrows represent the relative directions of the 30-kHz-wide sweeps used for excitation and storage. Notice the addition of gradient purging pulses to the schemes of Fig. 1. The central- and lower-panel spectra differ by the absence and presence of a 60-ms-long DIPSI-based mixing sequence[23] respectively. In all cases the 2D plots represent a positive description of the real $I(\nu_1, \nu_2)$ values, at a 7% lowest contour. [Correction made here after initial online publication]

Experiment and Modelling in Structural NMR Advanced Concepts - *Fast NMR*

J|A|C|S
ARTICLES
Published on Web 01/10/2007

UltraSOFAST HMQC NMR and the Repetitive Acquisition of 2D Protein Spectra at Hz Rates

Maayan Gal,† Paul Schanda,‡ Bernhard Brutscher,‡ and Lucio Frydman*,†

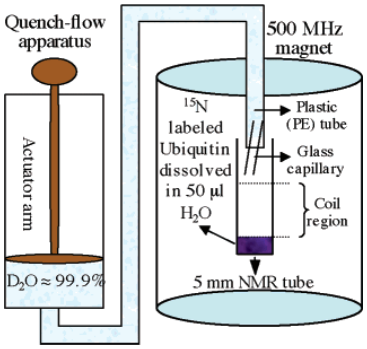

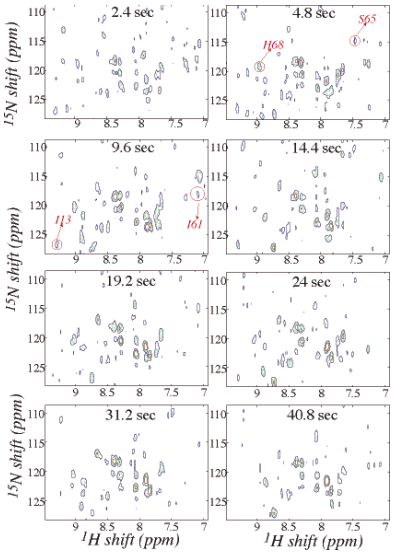

Figure 3. Representative series of real-time 2D ultraSOFAST HMQC NMR spectra recorded on a ⊠ 3 mM Ubiquitin solution, following the dissolution of an initially fully protonated lyophilized powder onto a D_2O-based buffer (final uncorrected pH) 8.9). The times indicated in each frame correspond to the approximate delay elapsed since the dissolution was suddenly triggered. Acquisition parameters were akin to those in Figure 2B (with N_{scan}) 8, T_{scan}) 250 ms) and so was the data processing. The repetition time between full recordings was ⊠ 2.4 s and data were monitored over a 20 min interval; only a subset of the collected and processed spectra is shown. The kinetics of the highlighted peaks are depicted by the corresponding graphs in Figure 4.

J|A|C|S
ARTICLES
Published on Web 01/10/2007

UltraSOFAST HMQC NMR and the Repetitive Acquisition of 2D Protein Spectra at Hz Rates

Maayan Gal,† Paul Schanda,‡ Bernhard Brutscher,‡ and Lucio Frydman*,†

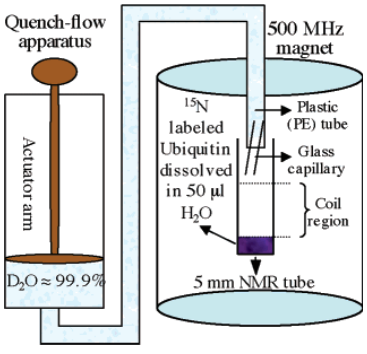

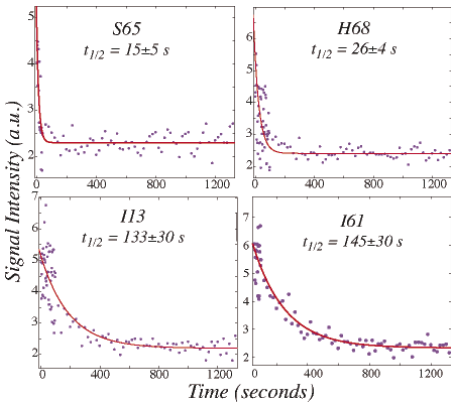

Figure 4. H/D exchange plots extracted from the data in Figure 3 for four residues exhibiting fast kinetic processes. Experimental points reflect peak heights in the ultraSOFAST HMQC 2D spectra; the $t_{1/2}$ exchange lifetimes given in the figure were obtained by fitting the data points to the equation $I(\tau)$) $I_e \exp(-\tau/t_{1/2}) + I_e$. The points chosen over the course of the first 50 measurements (time τ e 120 s) arise from full separate 2D acquisitions, each of these 2.4 s long. Thereafter, for the sake of reducing scattering and in view of the slowing down of the dynamics, ten consecutive spectra (50 through 60, 60 through 70, etc.) were co-added and the exchange time was assigned to the center time of this average. We ascribe the shorter lifetimes arising from these fits vis-à-vis their counterparts reported in ref 32, to the higher pH's (8.9 vs 6.5) in which measurements were now performed.

Experiment and Modelling in Structural NMR Advanced Concepts - *Fast NMR*

NMR Spectroscopy

DOI: 10.1002/anie.200902387

Real-Time Monitoring of Organic Reactions with Two-Dimensional Ultrafast TOCSY NMR Spectroscopy**

Antonio Herrera,* Encarnación Fernández-Valle, Roberto Martínez-Álvarez, Dolores Molero, Zulay D. Pardo, Elena Sáez, and Maayan Gal

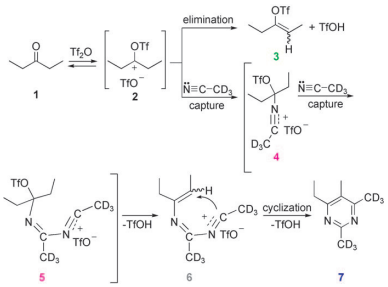

Scheme 1. The reaction between ketones and triflic anhydride in the presence of nitriles as nucleophiles.

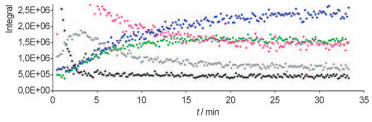

Figure 3. The averaged integrated peak intensity as a function of time for reactant 1 (▲), intermediates 4, 5 (▲), and 6 (▲), and final products 3 (▲) and 7 (▲).

Angew. Chem. Int. Ed.2009, 48, 6274 –6277

analytical chemistry

ARTICLE

pubs.acs.org/ac

Ultrafast Quantitative 2D NMR: An Efficient Tool for the Measurement of Specific Isotopic Enrichments in Complex Biological Mixtures

Patrick Giraudeau,*Stéphane Massou, Yoann Robin, Edern Cahoreau, Jean-Charles Portais, and Serge Akoka

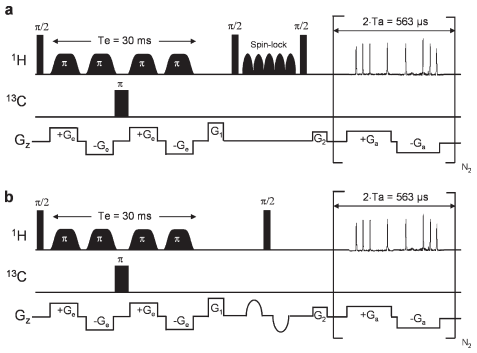

Figure 1. Pulse sequences for the acquisition of ultrafast zTOCSY (a) and COSY (b) spectra with 13C decoupling in the ultrafast dimension, using a phase-modulated encoding scheme of duration Te, followed by a mixing period and an EPI-based detection block. G1 and G2 gradients are adjusted for each sample to set the middle of the chemical shift range in the middle of the detection window.

analytical chemistry
ARTICLE
pubs.acs.org/ac

Ultrafast Quantitative 2D NMR: An Efficient Tool for the Measurement of Specific Isotopic Enrichments in Complex Biological Mixtures

Patrick Giraudeau,* Stéphane Massou, Yoann Robin, Edern Cahoreau, Jean-Charles Portais, and Serge Akoka

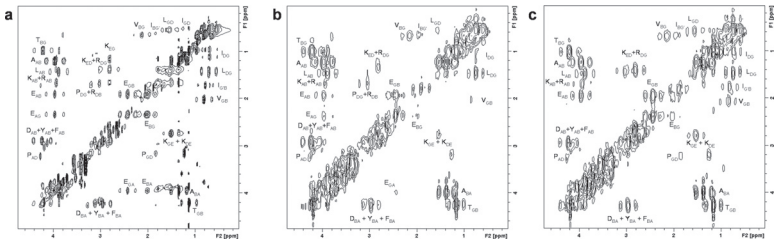

Figure 4. Conventional zTOCSY (a), ultrafast zTOCSY (b), and ultrafast COSY (c) spectra of a biomass hydrolyzate from E. coli cells grown on 50% of [U-^{13}C]-glucose and 50% of n.a. glucose. The sample contains mainly amino acids released from the hydrolysis of cellular proteins. The conventional spectrum was recorded in ca. 10 h, whereas the ultrafast spectra were acquired in 3 min (40 scans).

analytical chemistry
ARTICLE
pubs.acs.org/ac

Ultrafast Quantitative 2D NMR: An Efficient Tool for the Measurement of Specific Isotopic Enrichments in Complex Biological Mixtures

Patrick Giraudeau,* Stéphane Massou, Yoann Robin, Edern Cahoreau, Jean-Charles Portais, and Serge Akoka

^{1}H peak identifiers	conv zTOCSY (16 h)	UF zTOCSY (3 min)	UF COSY (3 min)
A_{AB}	44.5	45.7	41.2
A_{BA}	46.8	51.3	50.7
E_{AB}	47.9	44.7	45.2
E_{AG}	48.5	47.7	a
E_{BG}	48.7	b	b
E_{GB}	50.9	45.1	37.6
E_{GA}	49.7	b	a
I_{G^0B}	46.1	a	44.8
K_{EG}	44.6	a	a
L_{AB}	48.3	43.8	43.4
L_{DG}	47.9	42.7	45.1
P_{AD}	47.0	43.1	42.0
T_{BG}	26.9	23.0	25.8
T_{GB}	24.5	23.3	24.7
V_{GG^0}	47.9	42.3	47.6

[a] Quantification was not possible because the peak was absent from the 2D correlation. [b] Precise quantification was not possible due to overlap with other 2D peaks.

Experiment and Modelling in Structural NMR Advanced Concepts - *Fast NMR*

Gradient Frequency-Encoded

(gNMR) Spectroscopy

Sample Spatial Frequency Encoding: gNMR

Resolution vs Acquisition Rate: “Squaring the Circle”

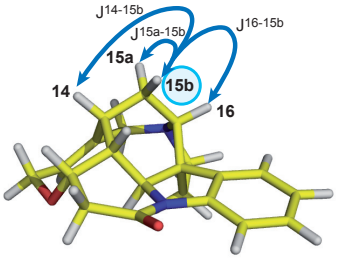

Strychnine

How to probe the spin network around H^{15b} ?

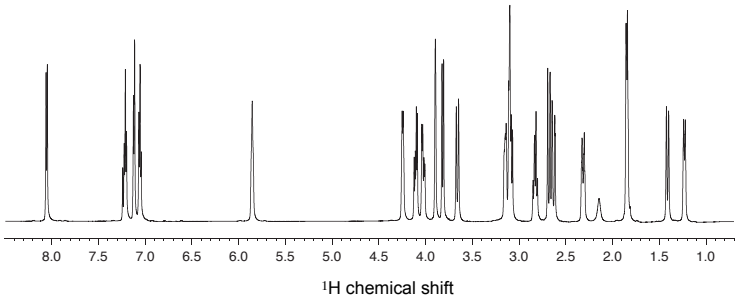

Sample Spatial Frequency Encoding: gNMR

Resolution vs Acquisition Rate: “Squaring the Circle”

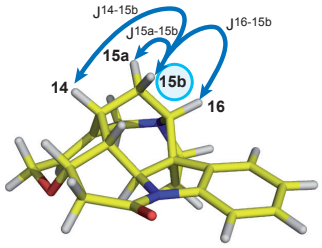

First approach : record multidimensional data

Dispersion of correlations along 2 spectral dimensions

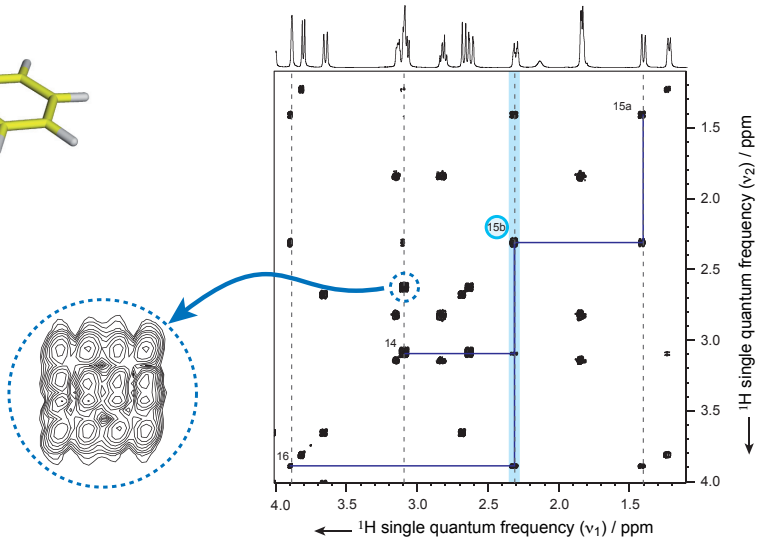

- Evolution of several spin interactions : line broadening
- Experimental time is limiting resolution / signal to noise ratio

Sample Spatial Frequency Encoding: gNMR

Resolution vs Acquisition Rate: “Squaring the Circle”

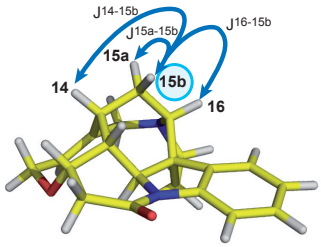

Second approach : refocus interactions

Only spin-spin interactions in the indirect domain

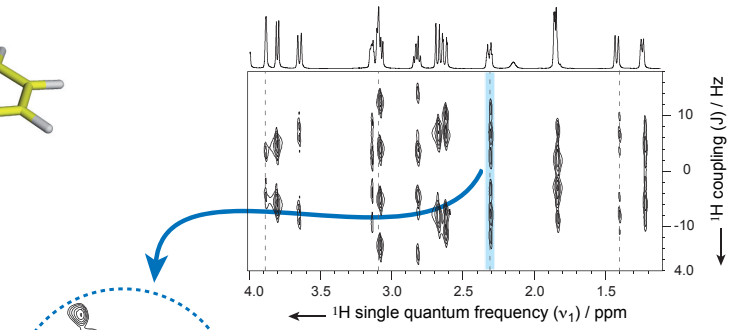

- Low resolution for fully coupled networks
- Several data sets have to be recorded to assign and measure every interactions
- Data analysis is a long process !

Sample Spatial Frequency Encoding: gNMR

Resolution vs Acquisition Rate: “Squaring the Circle”

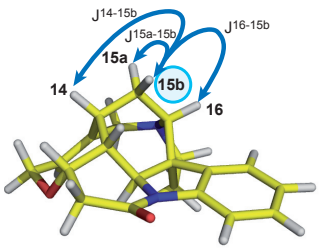

Third approach : selective refocusing

spin-spin interactions are selected by selective spin echoes

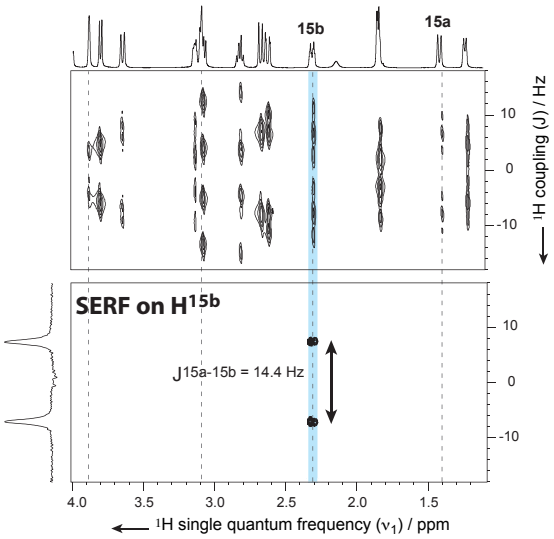

- A part of the analytical content is lost : where is the assignment ?!!
- Very long experimental time required to measure every coupling from large interaction networks

Sample Spatial Frequency Encoding: gNMR

Resolution vs Acquisition Rate: “Squaring the Circle”

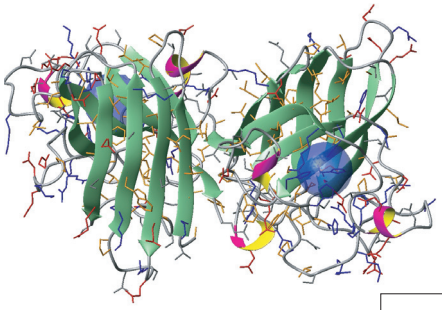

Human Dimeric Oxidized Cu(II), Zn(II) Superoxide Dismutase (SOD)

Fourth approach : combining hard and soft pulses

Works for some samples ...
(proteins - triple resonance experiments)

... not for fully coupled systems.

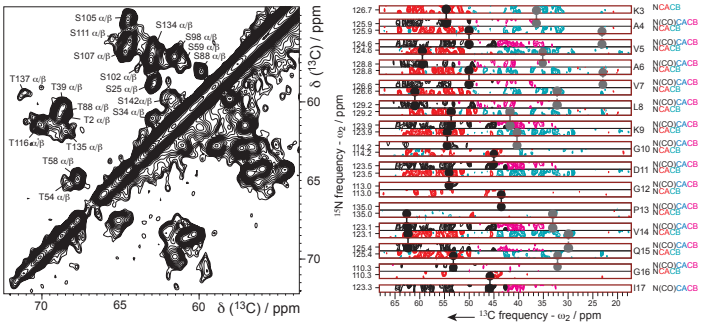

Pintacuda et al., Ang. Chem. Int. Ed. 46 (7): 1079-1082 (2007)

Experiment and Modelling in Structural NMR Advanced Concepts - *Fast NMR*

Sample Spatial Frequency Encoding: gNMR

Resolution vs Acquisition Rate: “Squaring the Circle”

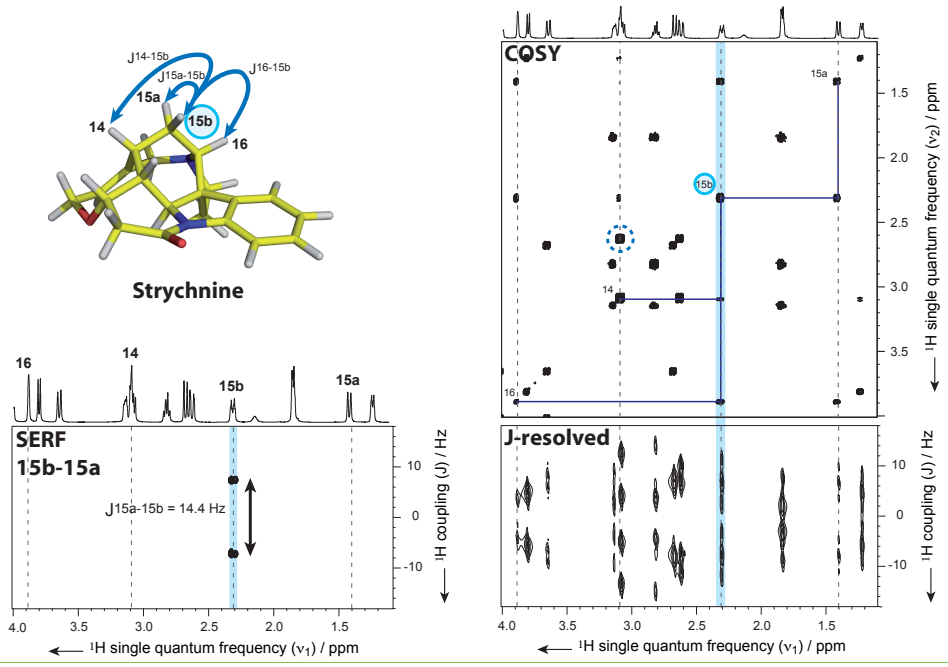

Sample Spatial Frequency Encoding: gNMR

Resolution vs Acquisition Rate: “Squaring the Circle”

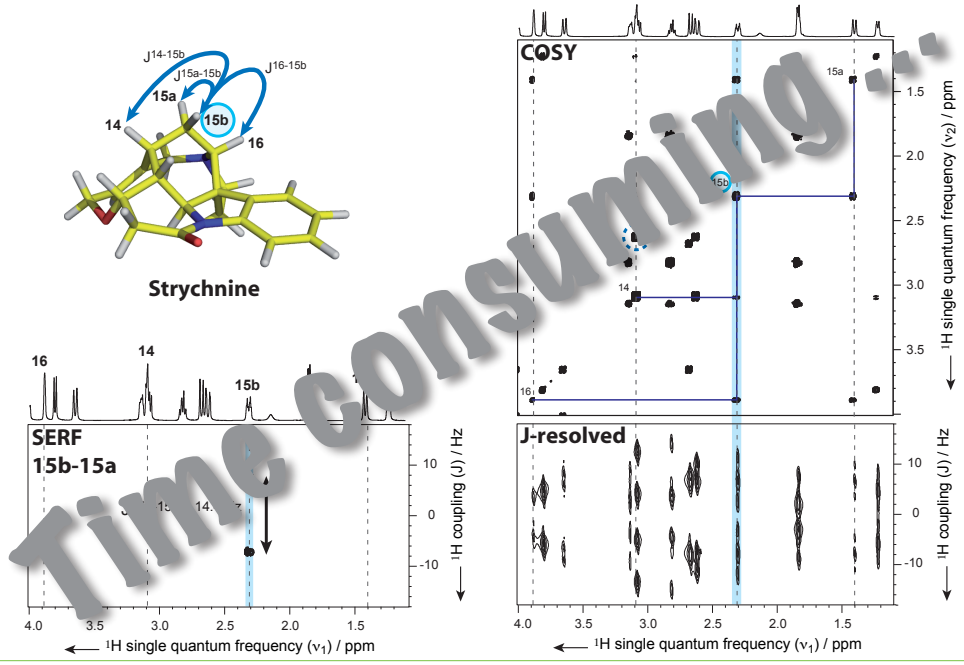

Time consuming...

Sample Spatial Frequency Encoding: gNMR

Resolution vs Acquisition Rate: “Squaring the Circle”

Network of *n* spins coupled together
(eg. ^{1}H spins in an anisotropic environment)

- *n* resonance frequencies ν^i
- up to *n(n-1)/2* spin-spin interactions
- overcrowded spectra !

Problem : State-of-the-art pulse sequences allow to handle nuclear spins either individually or all together ...

... what about handling simultaneously spin interactions ?...

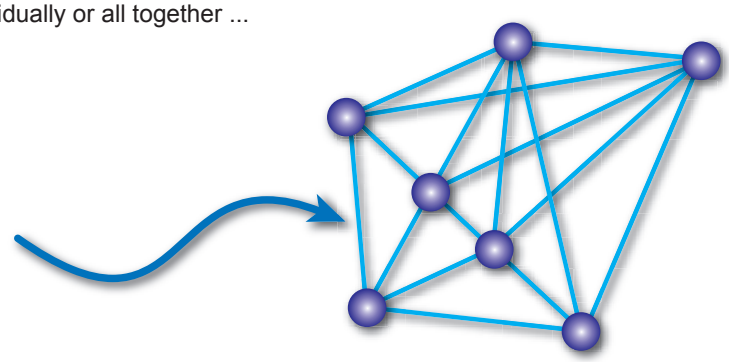

Sample Spatial Frequency Encoding: gNMR

Spatial Frequency Encoding Using A Pulsed Field Gradient

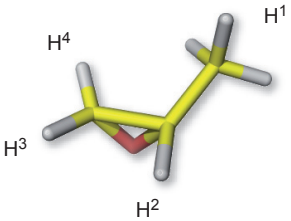

Propylene Oxide

Sample Spatial Frequency Encoding: gNMR

Spatial Frequency Encoding Using A Pulsed Field Gradient

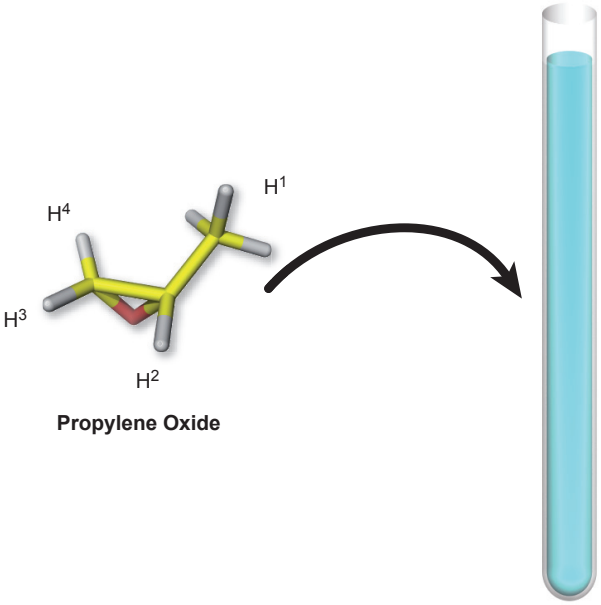

Sample Spatial Frequency Encoding: gNMR

Spatial Frequency Encoding Using A Pulsed Field Gradient

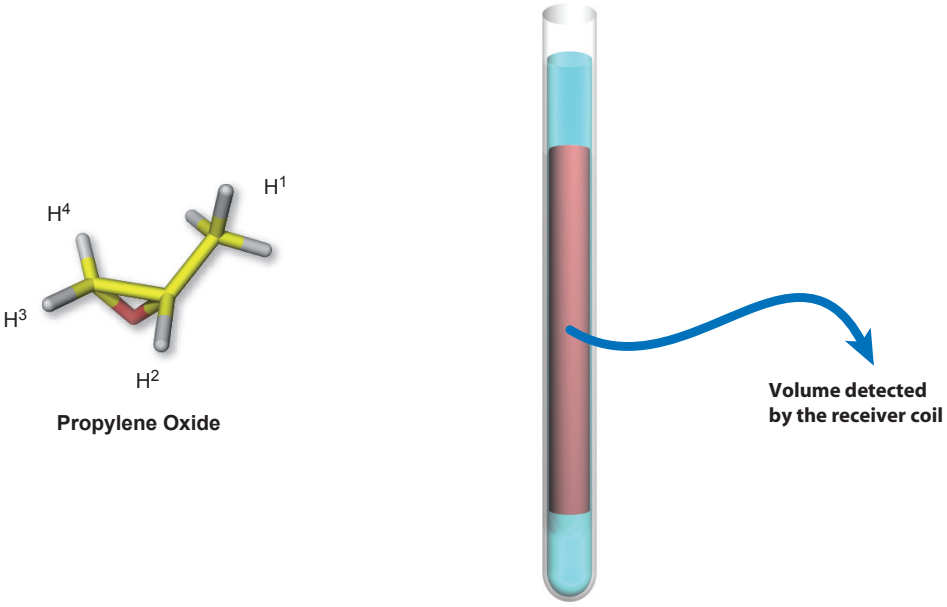

Experiment and Modelling in Structural NMR Advanced Concepts - *Fast NMR*

Sample Spatial Frequency Encoding: gNMR

Spatial Frequency Encoding Using A Pulsed Field Gradient

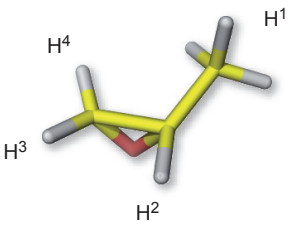

Propylene Oxide

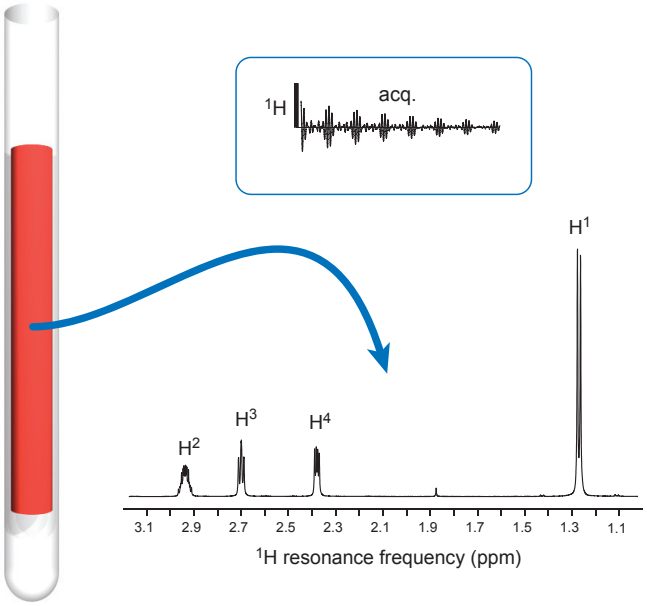

Broadband excitation of all the proton sites over the whole sample

Sample Spatial Frequency Encoding: gNMR

Spatial Frequency Encoding Using A Pulsed Field Gradient

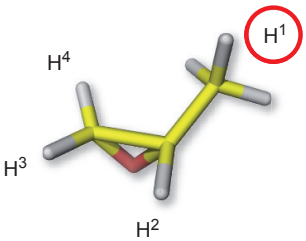

Propylene Oxide

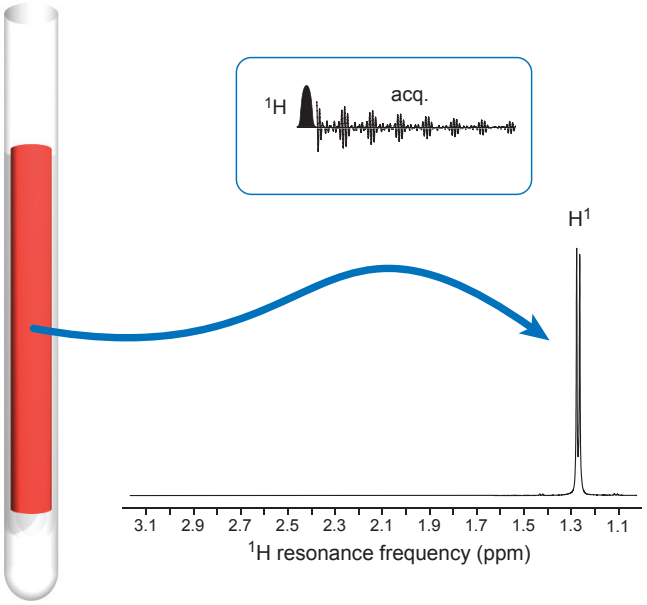

Semi-selective excitation of H^1 proton site over the whole sample

Experiment and Modelling in Structural NMR Advanced Concepts - *Fast NMR*

Sample Spatial Frequency Encoding: gNMR

Spatial Frequency Encoding Using A Pulsed Field Gradient

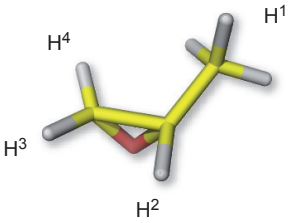

Propylene Oxide

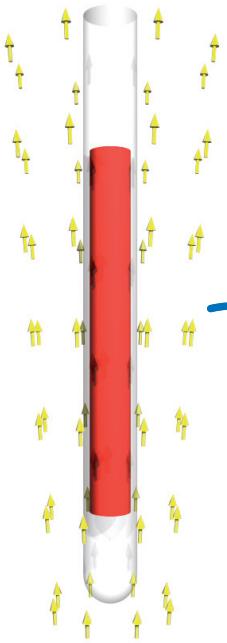

Application of a Pulsed Field Gradient

Sample Spatial Frequency Encoding: gNMR

Spatial Frequency Encoding Using A Pulsed Field Gradient

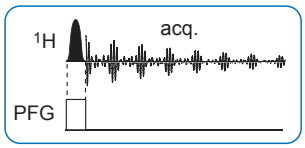

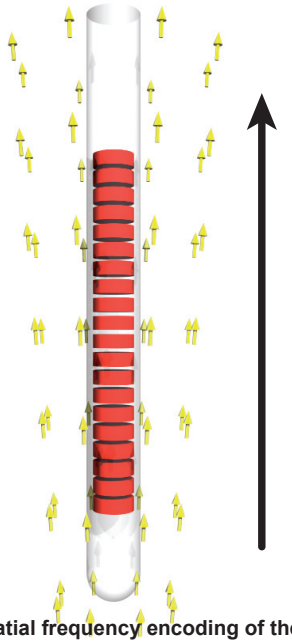

$$\nu(z) = \gamma B(z)/2\pi$$

Creation of a spatial frequency encoding of the sample

Sample Spatial Frequency Encoding: gNMR

Spatial Frequency Encoding Using A Pulsed Field Gradient

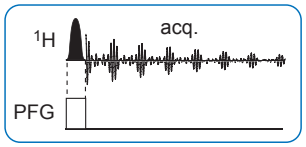

Proton spins with different resonance frequencies are excited in different "slices" of the sample

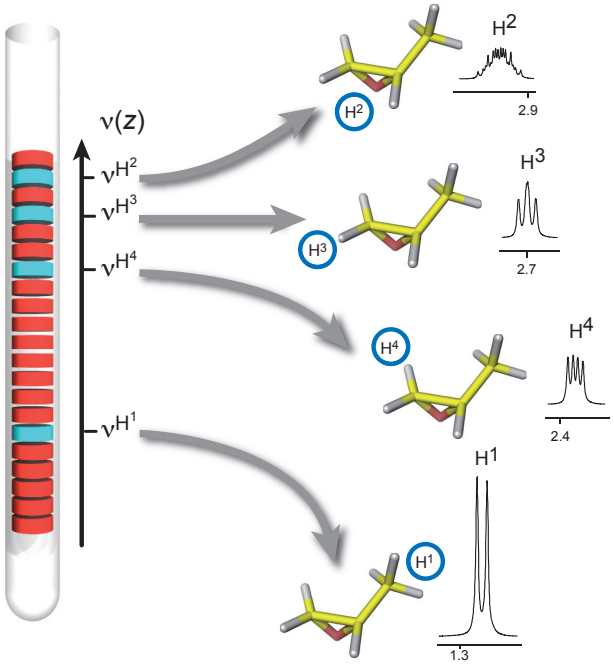

Sample Spatial Frequency Encoding: gNMR

Spatial Frequency Encoding Using A Pulsed Field Gradient

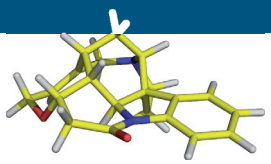

Spatially encoded ^{1}H spectrum recorded on strychnine

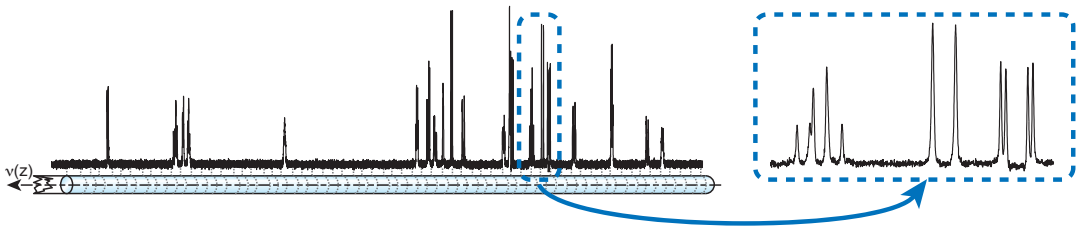

Broadband excitation ^{1}H spectrum

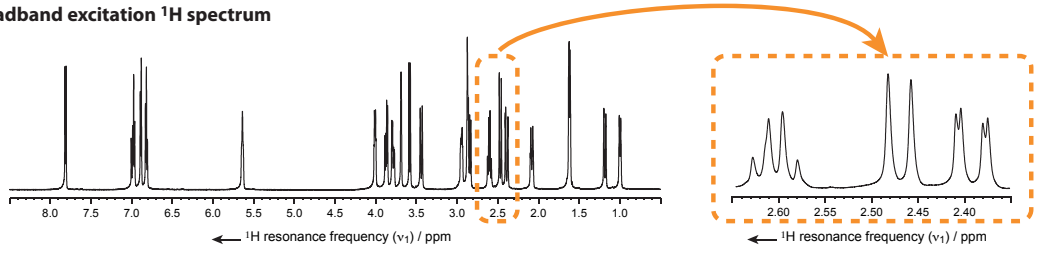

Giraud et al., Angew. Chem. Int. Ed. 2010, 49, 3481 –3484

Experiment and Modelling in Structural NMR Advanced Concepts - *Fast NMR*

Sample Spatial Frequency Encoding: gNMR

J-Edited Spectroscopy: The G-SERF Experiment

G-SERF: Gradient-encoded SElective ReFocusing spectroscopy

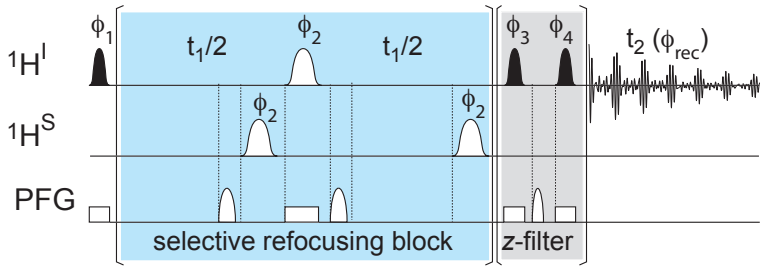

Giraud et al., Angew. Chem. Int. Ed. 2010, 49, 3481 –3484

Sample Spatial Frequency Encoding: gNMR

J-Edited Spectroscopy: The G-SERF Experiment

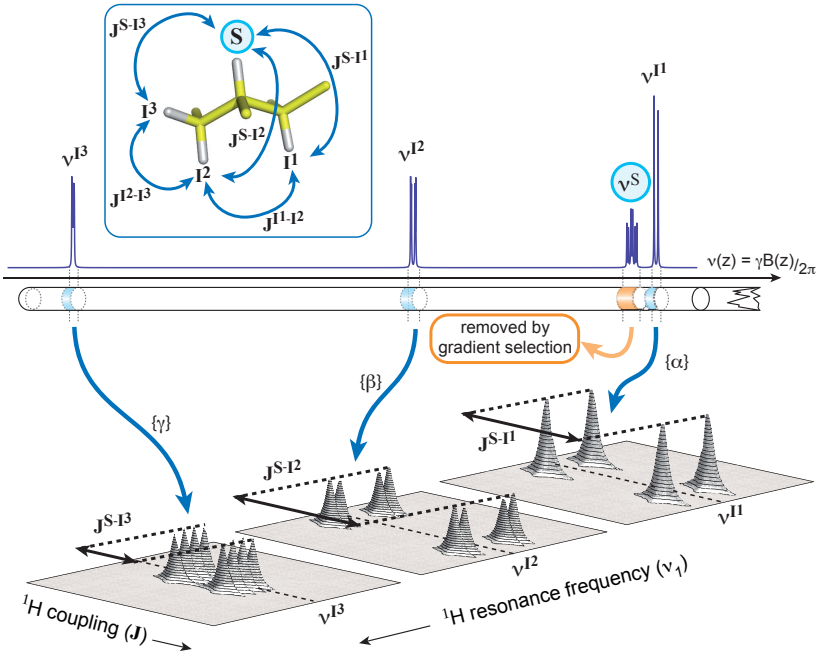

Experiment and Modelling in Structural NMR Advanced Concepts - *Fast NMR*

Sample Spatial Frequency Encoding: gNMR

J-Edited Spectroscopy: The G-SERF Experiment

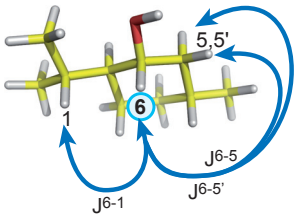

Menthol

- simple measurement, in the indirect domain, of all the scalar couplings involving H^6.

- direct assignment, in the direct domain, of the coupling network of H^6.

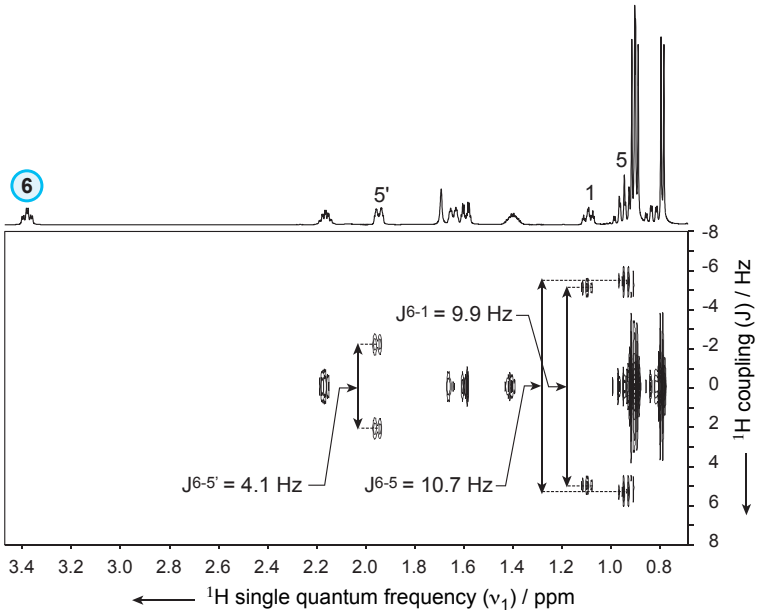

Sample Spatial Frequency Encoding: gNMR

J-Edited Spectroscopy: The G-SERF Experiment

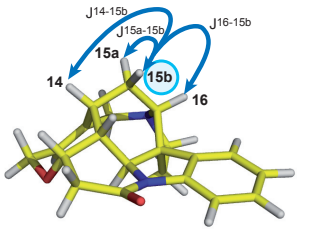

Strychnine

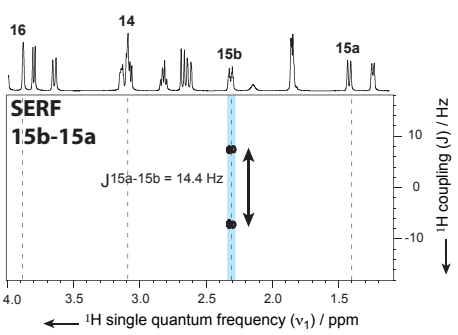

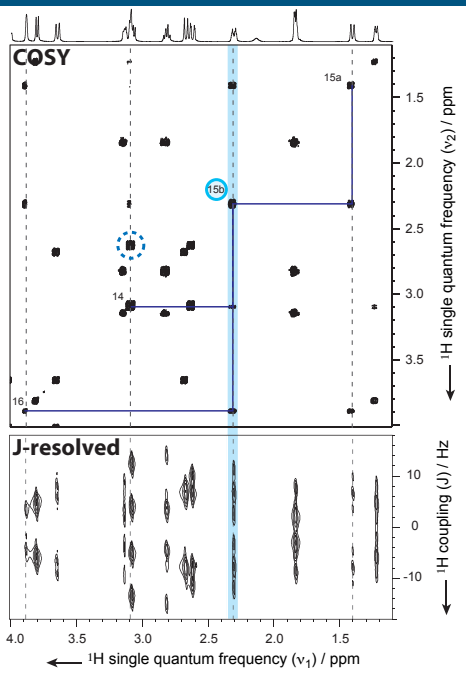

Sample Spatial Frequency Encoding: gNMR

J-Edited Spectroscopy: The G-SERF Experiment

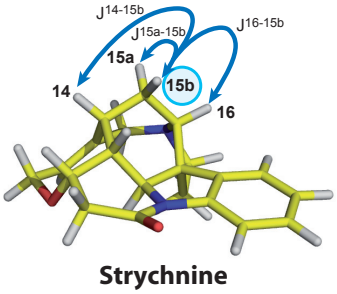

Strychnine

The proton network around H^{15b} can be straightforwardly assigned and measured, in a *single* G-SERF experiment.

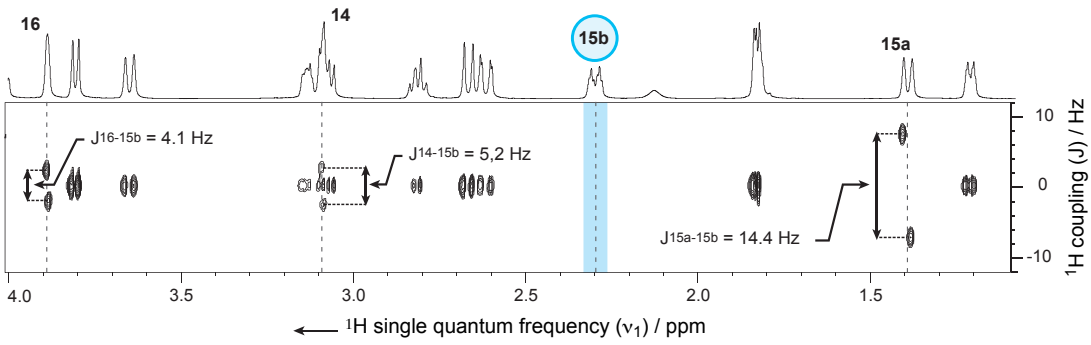

Sample Spatial Frequency Encoding: gNMR

J-Edited Spectroscopy: The G-SERF Experiment

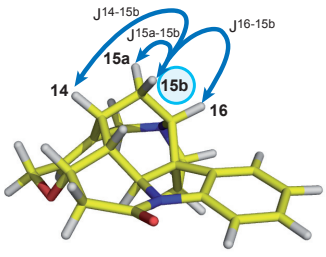

Strychnine

The conventional *J-resolved* spectrum provides chemists with complex multiplet structures that require additional data in order to be exploited.

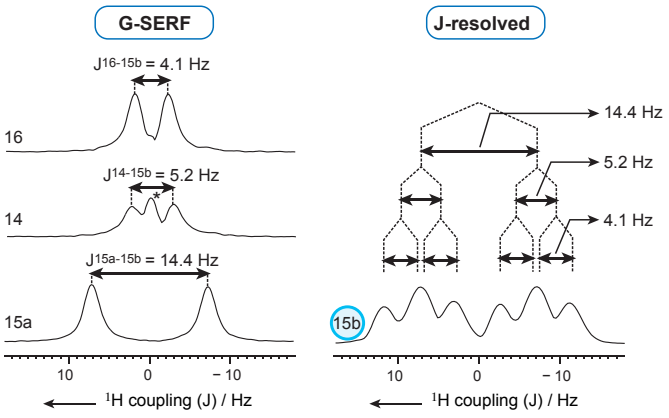

Sample Spatial Frequency Encoding: gNMR

Application to NMR in Chiral Liquid Crystal Solvent

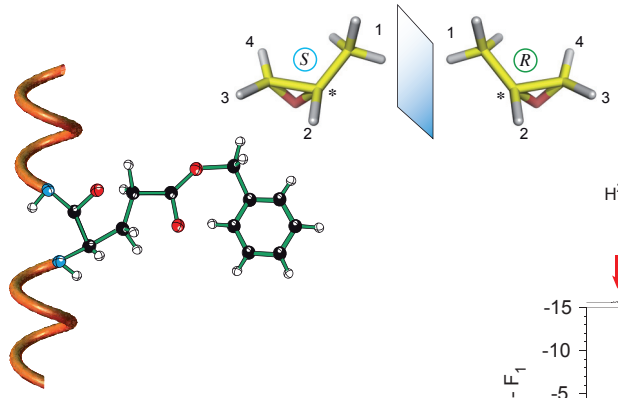

- 55 mg of $R+S$ propylene oxide (e.e. ~ 25 %)
- solvent : PBLG / $CDCl_3$
- t_1^{max} = 3.84 s / t_2 = 2 s
- NS = 8
- spectrum recorded in 10.5 hours

G-SERFph proton 2D spectrum recorded on propylene oxide dissolved in PBLG

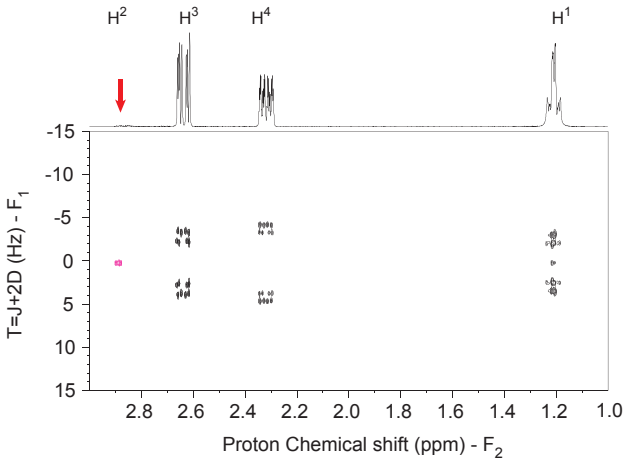

Sample Spatial Frequency Encoding: gNMR

Application to NMR in Chiral Liquid Crystal Solvent

The couplings which are measured straightforwardly on the G-SERFph spectrum allow to fully interpret the analogous multiplet extracted from a classical J-resolved experiement.

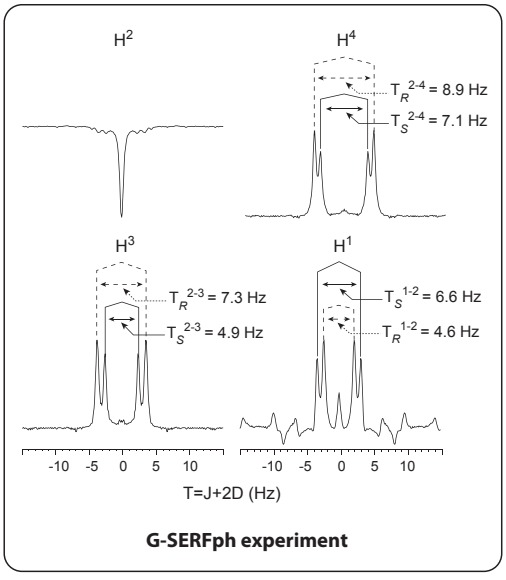

G-SERFph experiment

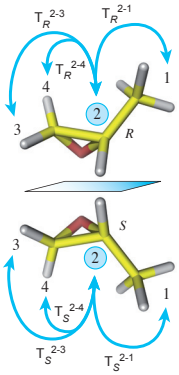

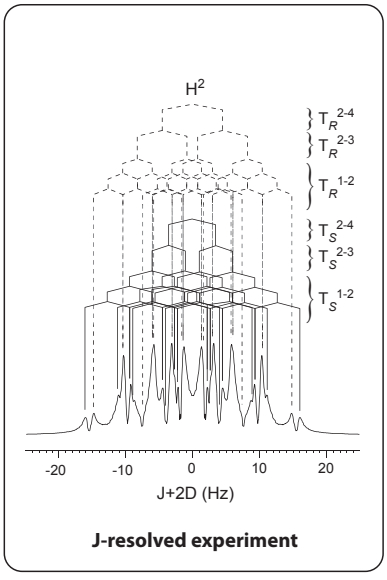

J-resolved experiment

Sample Spatial Frequency Encoding: gNMR

Application to NMR in Chiral Liquid Crystal Solvent

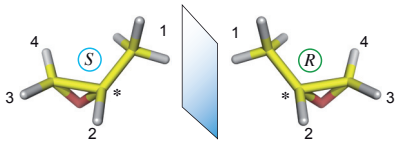

The same couplings involving the coupling network around H^1 in propylene oxide, can be extracted from:

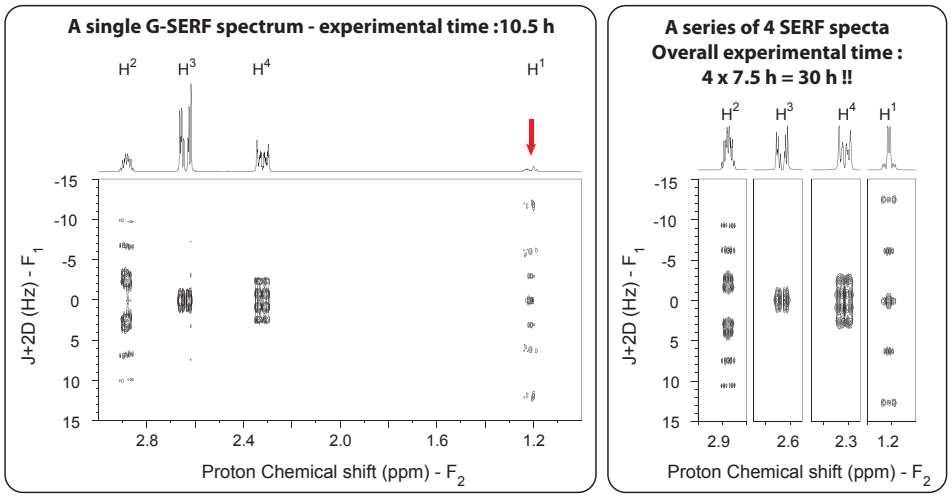

Sample Spatial Frequency Encoding: gNMR

J-Edited Spectroscopy: The G-SERF Experiment

A less sensitive but credible way of accelerating analysis of coupled systems ...

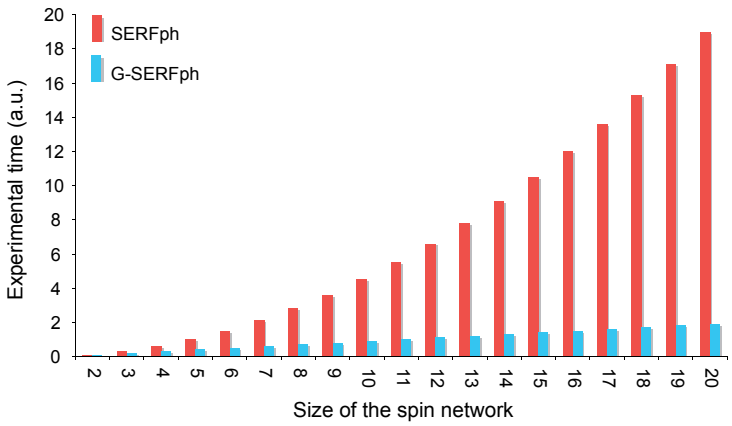

- Experimental time mainly limited by the number of scans, and the number of points in the indirect domain,
- Very high fields and/or cryo-probes can nowadays address sensitivity issues efficiently,
- The analytical content is much easier to extract.

Merlet et al., J. Magn. Res. 209 (2): 315-322 (2011)

Aknowledgements

SOFAST NMR : Bernard Brutscher, Ewen Lescop, Paul Schanda and coworkers

Ultra-Fast NMR : Lucio Frydman, Philippe Pelupessy, Patrick Giraudeau, Yoav Shrot, Assaf Tal and coworkers ...

gNMR : Nicolas Giraud, Denis Merlet and coworkers ...